E82-10002

SDSU-RSI-81-11

REMOTE SENSING APPLICATIONS TO RESOURCE PROBLEMS IN SOUTH DAKOTA

For

National Aeronautics and Space Administration
Office of University Affairs
Washington, D.C.

1 July 1980 to 30 June 1981

Annual Progress Report

Grant No. NGL 42-003-007

rsi REMOTE SENSING INSTITUTE

SOUTH DAKOTA STATE UNIVERSITY
BROOKINGS, SOUTH DAKOTA, U.S.A.
57007

E82-10002

SDSU-RSI-81-11

CR-164892

REMOTE SENSING APPLICATIONS TO RESOURCE PROBLEMS IN SOUTH DAKOTA

Principle Investigator

Victor I. Myers

Contributors:

T. Bailey
R. G. Best
J. C. Eidenshink
D. Hause
H. Haivala
F. A. Schmer
M. Wehde
K. Winks

For:

National Aeronautics and Space Administration
Office of University Affairs
Washington, D.C.

1 July 1980 to 30 June 1981

Annual Progress Report

Grant No. NGL 42-003-007

FORWARD

This manuscript is a collection of 7 annual (1 July 1980 - 30 June 1981) progress reports entitled: "Application of Remote Sensing for Sage Grouse Management in South Dakota"; "Computerized Digitization of Aerial Thermal Infrared Data for Censusing Canada Geese"; "Utilization of Landsat Data for Monitoring Grasshopper Infestation in Rangeland"; "Application of Remote Sensing Techniques for Dutch Elm Disease Detection in an Urban Environment"; "Determination of Water Usage From the Belle Fourche River"; "Resource Management of the Lower James River"; and "Application of Remote Sensing in the Model Implementation Program - Lake Herman Watershed". These projects were funded (NASA Grant NGL 42-003-007) under a common proposal entitled "Remote Sensing Applications to Resource Problems in South Dakota", V. I. Myers, Principal Investigator.

TABLE OF CONTENTS

TABLE OF CONTENTS - Continued

TABLE OF CONTENTS - Continued

LIST OF FIGURES

LIST OF FIGURES - Continued

LIST OF FIGURES - Continued

LIST OF TABLES

APPLICATION OF REMOTE SENSING FOR SAGE GROUSE MANAGEMENT IN SOUTH DAKOTA

By

R. G. Best, T. Bailey, H. Haivala and T. Schenck

ABSTRACT

South Dakota has a small huntable population of sage grouse in the western counties. Only a limited amount of data is available on sage grouse habitat or the factors limiting the population and distribution of sage grouse in South Dakota. The objective of this project is to evaluate the use of remotely-sensed imagery in sage grouse management programs. Sagebrush is a primary component of both nesting and brooding habitat and winter habitat. Field data, including crown coverage, density and height and breadth, of sage brush were collected within a 3 Km radius of known active leks. These data not only determine sage grouse habitat usage, but also will affect the appearance of the habitat on imagery. Ground level color-infrared photos illustrate the lack of a characteristic red reflectance for big or silver sage brush. Sagebrush/grassland communities can most accurately be interpreted on color-infrared aerial photography collected during vegetative "peak green" at scales 1:20,000 or greater. A sage grouse management potential map based on interpretations of land use and ownership from small scale imagery was prepared for Harding County, South Dakota. Interpretations of winter Landsat imagery confirmed that winter habitat may be a major limiting factor for the sage grouse population in South Dakota.

APPLICATION OF REMOTE SENSING FOR SAGE GROUSE MANAGEMENT IN SOUTH DAKOTA

By

R. G. Best, T. Bailey, H. Haivala and T. Schenck[1/]

INTRODUCTION

The sage grouse or sage hen, *Centrocercus urophasianus*, once ranged across 15 western states and was considered the leading upland game bird in nine (Rasmussen and Griner 1938). The sage grouse is the largest North American grouse with males often weighing as much as 2.7 Kg (6 lbs.). There has been a continuing destruction of sage grouse habitat because of improvements in agricultural technology resulting in agricultural encroachment and increased domestic livestock grazing. At present, sage grouse are hunted in 11 states but are a major game bird in only three, Idaho, Montana, and Wyoming (June 1969). South Dakota has a small population in 4 counties (Harding, Butte, Perkins, and Fall River) located along the western edge of the state. Hunting of sage grouse in South Dakota has been limited to a three-day season with restricted bag limits as a result of a lack of knowledge of the population size and exact distribution. Furthermore, very little is known of the current trend of sage grouse habitat changes in the state. There is a growing concern, by game biologists, on the effect of continued alteration of the sagebrush-grassland on sage grouse populations.

[1/]Wildlife Specialist, Remote Sensing Institute, South Dakota State University, Brookings, South Dakota; Conservation Officers, Harding and Butte Counties, and Assistant Regional Supervisor, South Dakota Department of Game, Fish and Parks, respectively.

Sage grouse inhabit the semi-arid northern desert scrub areas, the mixed and short grass plains and the mountain parks where sagebrush (*Artemisia* sp.) is a climax vegetation species (Aldrich 1963). Sagebrush is a primary component of nesting and brooding habitat. Sage grouse are totally dependent on sagebrush for cover and food during the winter months from October to April (Rasmussen and Griner 1938, Patterson 1952, Eng and Schadweiler 1972, Wallestad et al. 1975). During winters with above normal snowfall much of the sagebrush wintering areas may be covered with snow placing severe stress on grouse populations. A method for yearly monitoring of winter cover can be very useful for determining the effects of winter on sage grouse populations.

Two species of sagebrush, silver sagebrush (*Artemisia cana*) and big sagebrush (*A. tridentata*) are present throughout the sage grouse range in South Dakota (Johnson and Nichols 1970). The silver sagebrush normally grows from 1-1.6 m (3-5 ft.) tall. The big sagebrush grows to heights of 1 m (3 ft.) south of the Black Hills, but is seldom over 45.7 cm (18 in.) tall in Harding and Butte Counties (Johnson and Nichols 1970). Both species maintain their foliage throughout the winter months. Procedures for identifying areas of vegetation emerging through snow cover (i.e. wetland vegetation, trees, riparian)in the ring-necked pheasant (*Phasianus colchicus*) range of eastern South Dakota were developed and illustrated in a previous NASA project (Best and Sather-Blair 1978, Best and Solomon 1979). It is reasonable to assume that within the resolution of Landsat, sagebrush emerging through snow cover should provide sufficient spectral contrast to be interpretable on Landsat imagery.

Poulton (1975) summarizes numerous applications of remotely sensed data in range and wildlife habitat management. Carnegie (1968) lists the general types of range data which can be interpreted from color and color infrared imagery when combined with field investigations including (1) delineating and classifying plant communities and their associated soils, and (2) determining species composition and foliage density of dominant shrubs, grasses and herbs. Carnegie illustrates the interpretation of big sagebrush on color and color-infrared imagery collected in early June.

Currently, sage grouse managers rely on ground surveys to determine the extent and quality of habitat for wintering and nesting sage grouse. The use of remotely-sensed imagery may provide a method for accurately determining the distribution of habitat for large areas in a relatively short time. Landsat imagery are particularly suited for temporal monitoring of wintering habitat which may be an important population limiting factor in the South Dakota sage grouse range.

The objectives of this project were (1) develop an operational use of remotely-sensed data for sage grouse management in South Dakota; (2) evaluate the use of snow cover Landsat imagery for determing the distribution of and for monitoring yearly changes in available sage grouse winter habitat; (3) evaluate the use of aerial photographs for determining the distribution of nesting and brooding habitat; and (4) document and illustrate the techniques that are developed and transfer the appropriate technology to South Dakota Department of Game, Fish and Parks personnel.

PROCEDURES

Six 6.5-9.5 square kilometer test sites centered around active leks (strutting grounds) were selected to develop interpretation procedures (Figure 1). Three other smaller test sites with sage grouse present but with the lek site unknown were also selected. Extensive ground data collection was completed on these test sites to determine sage grouse habitat requirements and for ground truth to develop image interpretation criteria.

Collection of Remotely Sensed Imagery

High altitude color infrared imagery (scale = 1:120,000) of Harding County was collected by NASA on 29 April 1980. Data were originally scheduled for collection during late May or June of the same year. Existing color-infrared imagery of Butte County collected by NASA on 25 June 1975 were used to supplement the Harding County imagery. This imagery was collected during vegetative "peak green" and may show better infrared contrast in the vegetation types making up sage grouse habitat. Black and white ASCS aerial photographs (1:15,800) collected 25 June 1980 were acquired for Butte County test sites. Color (2448), color infrared (2443) and black and white panchromatic (2402) aerial photography was collected simultaneously at scales of approximately 1:15,000 and 1:58,000 for Butte County test sites on 3 June 1980. Winter Landsat scenes covering Harding, Butte, Perkins and Fall River Counties were acquired for ten dates between 1973 and 1980 (Table 1). These dates represent a variety of snowcover conditions during the past 8 winter seasons.

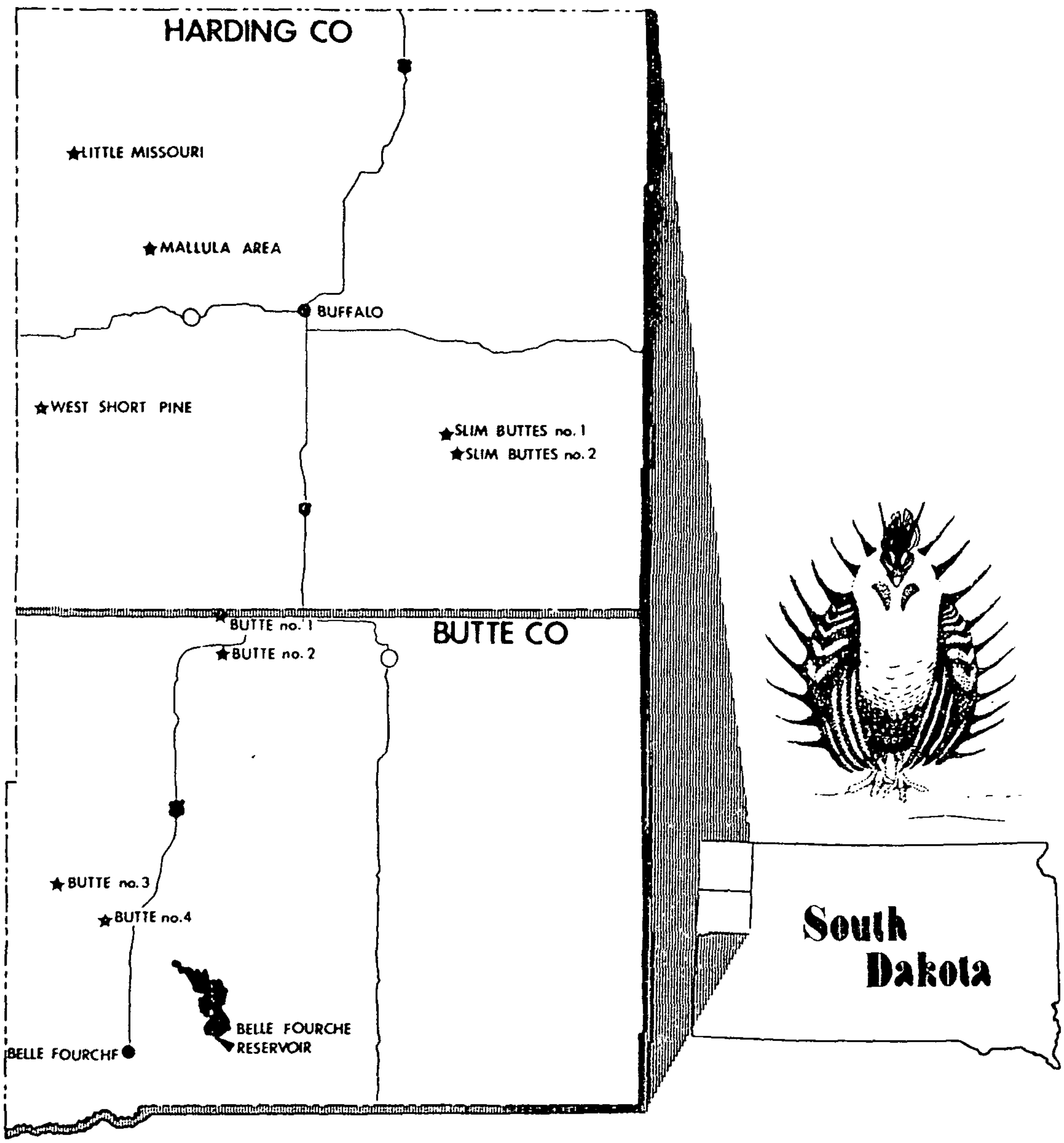

Figure 1. Location of field data collection sites in Harding and Butte County, South Dakota.

Table 1. Winter Landsat imagery acquired for sage grouse winter habitat interpretation.

Date	Snowfall on Ground (in.)
11 January 1980	0-3
7 January 1979	3-12
14 November 1978	3-12
17 February 1978	>12
30 January 1978	6-12
30 December 1976	3-12
18 December 1975	3-6
24 February 1975	1-12
19 December 1973	1-6
11 January 1973	6-12

Collection of Field and Ancillary Data

A review of related literature indicated that the factors (i.e. crown cover, density, height, species) that determine sage grouse habitat usage also affect the appearance of the habitat on imagery. All field measurements were done with standard procedures in order to correlate the habitat data collected in this project with results of other reported studies. Forty-six vegetational transects were taken within 3 Km (2 mi.) radius of six known active sage grouse leks in Harding and Butte Counties, South Dakota. A complete listing of field data was presented in the Semi-Annual Report (Best et al. 1981). Wallestad and Pyrah (1974) found that 68% of all nests in a non-migratory population of sage grouse occurred within a 2.5 Km (1.5 mi.) radius of leks. The percent canopy coverage of big

sage, silver sage, grasses and forbs, and percent bare soil were visually estimated and recorded by classes according to methods developed by Daubenmire (1959). The percentage canopy cover of forbs was included with grasses but the presence of forbs was also noted. The average percentage canopy cover for each transect was calculated as the average of the means of the six coverage classes present. The total canopy coverage can vary slightly from 100% in this method.

The height and crown breadth of big and silver sage were calculated as averages of measurements of 20 consecutive plants along the transect. The density of both big and silver sage are an average of 2 counts of all plants in a 40 square meter plot laid out parallel to the transect. The slope of each transect was measured with a clinometer and aspect determined with a compass. The mean cover value was calculated as the product of average height and density in a method used by Beck (1977).

Color-infrared and Ektachrome photos of each transect, the leks and surrounding landscape were also collected. Any evidence of sage grouse use in an area (i.e. presence of droppings or visual observations), were recorded with notes on grazing and other pertinent facts.

Contour maps of snow cover corresponding to the dates of Landsat data acquisition were produced using SYMAP software developed at Harvard (Dougenek and Sheehan 1977). Snow depth were encoded from reports provided from the State weather monitoring network. Output from the system includes computer overstrike maps and color encoded displays produced via RSI's Signal Analysis and Dissemination Equipment (SADE).

RESULTS AND DISCUSSION

Sagebrush is the primary component of nesting and brooding habitat as well as winter habitat. The slope, type and density of vegetation, and the distance from strutting ground all have an influence on the nesting location and success (Patterson 1952, Klebenow 1969, Wallestad and Pyrah 1974). These investigators have found that nearly all sage grouse nests are located under sagebrush where total shrub cover exceeds 15% and always averaged less than 35%. They have reported an average sagebrush height of approximately 40.6 cm (16 in.) at nesting sites. Furthermore, the largest percentage of nesting occurs within 3 Km of a lek. Field data indicated that sage grouse were not selectively utilizing one species of sagebrush over the other in South Dakota and sagebrush canopy coverage was considered as the sum of both silver and big sage in mixed stands. The field data collected in this project indicated that in general, sufficient sagebrush canopy cover was present at nesting sites in the South Dakota sage grouse range but that in most cases the height of the sagebrush was much less than the average reported by other investigators in the primary sage grouse range. (See Appendix A).

Brooding occurs in less dense stands of sagebrush with many juveniles moving into native hay or cultivated areas after 6 to 8 weeks of age (Eng 1952, Rogers 1964). Grouse may utilize a more mesic site, such as creek bottoms during late summer (Wallestad 1971). Food studies indicate a high usage of forbs and varying amounts of animal matter by adult and juvenile sage grouse during summer months (Klebenow and Gray 1968,

Peterson 1970, Wallestad et al. 1975). Broods move into alfalfa fields to feed in late June when native forbs begin to cure. The field data indicate that adequate amounts of native forbs are present throughout most of the study area.

Neither big nor silver sagebrush exhibited the characteristic bright red tones of actively growing vegetation when they were photographed with 35 mm color-infrared film during field data collection. This may result in better contrast with range grasses during vegetative "peak green" but less contrast during periods when grasses are not actively growing. Subtle differences between stands of sagebrush and range grasses are evident on the small scale 1:120,000 color infrared imagery collected in June (Figure 2). The sagebrush stands have a dark bluish-red mottled appearance on the imagery. The areas that have the darkest tones are areas of highest sagebrush density. The 2 species of sagebrush could not be differentiated. Silver sage most commonly occurs on more mesic areas.

Sagebrush could not be interpreted on the small scale imagery collected in May 1980. This may result from a combination of factors including the spatial resolution of the imagery and the lack of spectral differences between the sagebrush and surrounding grassland because of the early date of data collection and the drought conditions experienced throughout 1980. Several investigators have been successful in interpreting sagebrush communities on small scale aerial photography (Driscoll et al. 1974, Batson and Elliot 1975). Driscoll et al. (1974) used a micro densitometer in order to optimize the discrimination of plant communities on high altitude color infrared imagery. Batson and Elliot (1975) photo-interpreted

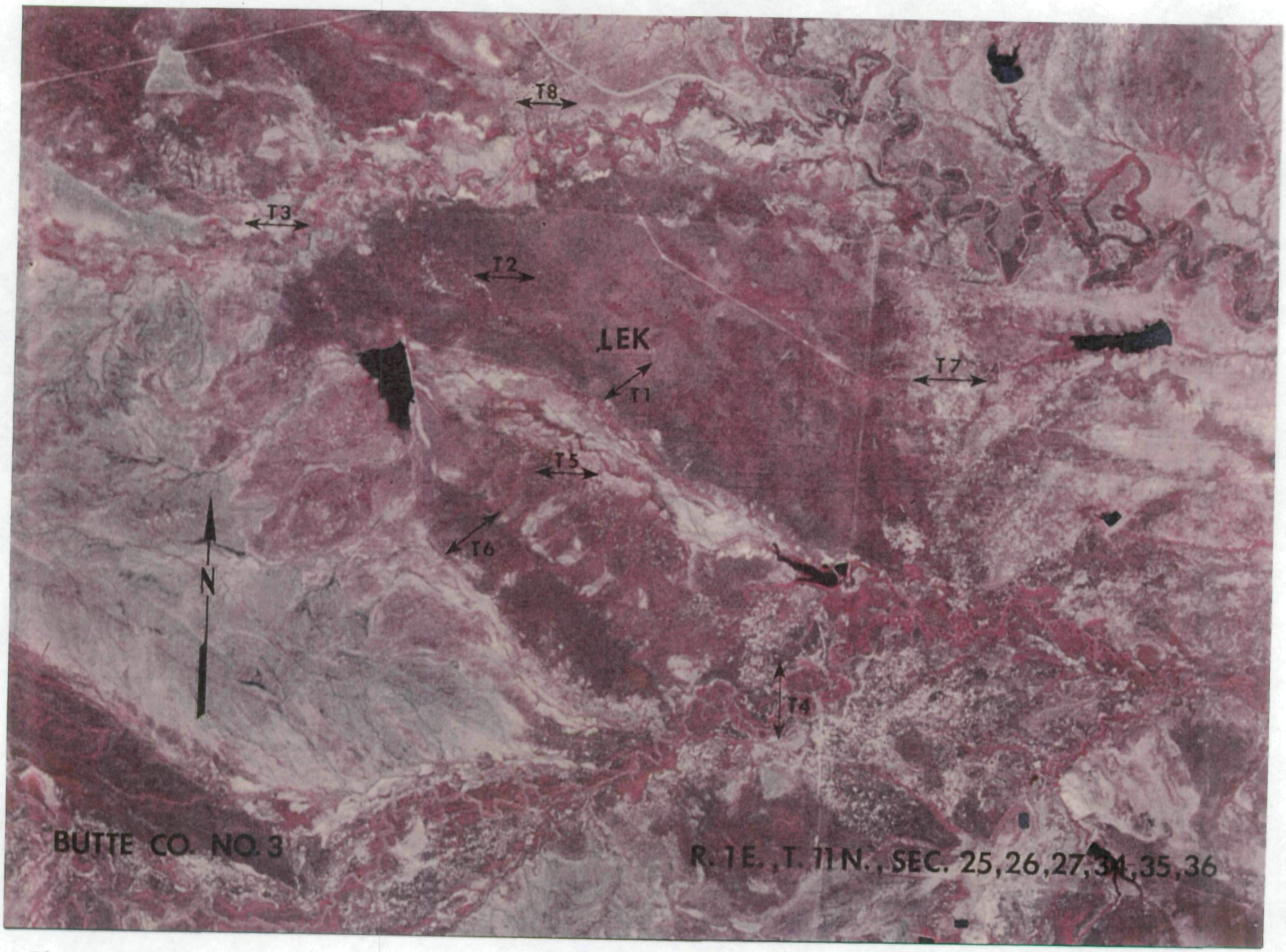

Figure 2. High altitude color-infrared aerial photo of Butte County, No. 3 test site (scale = 1:24,000).

and mapped grassland, shrub and tree communities on 1:80,000 color infrared imagery collected during peak green. They were able to distinguish both silver sagebrush/grassland and big sagebrush/grassland type communities. They established a numerical rating for each vegetation type based on its potential for wildlife habitat.

The grassland communities could easily be distinguished from the cultivated and forested areas on the small scale imagery collected both in April and June. These data when used in combination with land ownership maps and field data were used to produce a sage grouse management potential map for Harding County South Dakota (Figure 3). The red areas on the map are publicly owned rangelands which would have the greatest management potential. The yellow areas are privately owned rangeland for which management can only be suggested to the owners. The green areas are cultivated with little or no value as sage grouse habitat when they occur in large blocks as in the northeast portion of the county. They can provide valuable late summer brood habitat when interspersed with the sagebrush/grassland community.

The interpretation of the sagebrush communities was greatly simplified on the larger scale (1:15,000) aerial photography collected 3 June 1981 (Figure 4). The color film had the greatest contrast between sagebrush and grassland. The black and white panchromatic photograph also showed enough contrast for accurate delineation of sagebrush. The color-infrared imagery had the least vegetative contrast which can be attributed to a lack of actively growing grasses resulting from a second consecutive year of drought. Differences in stand density and crown coverage were

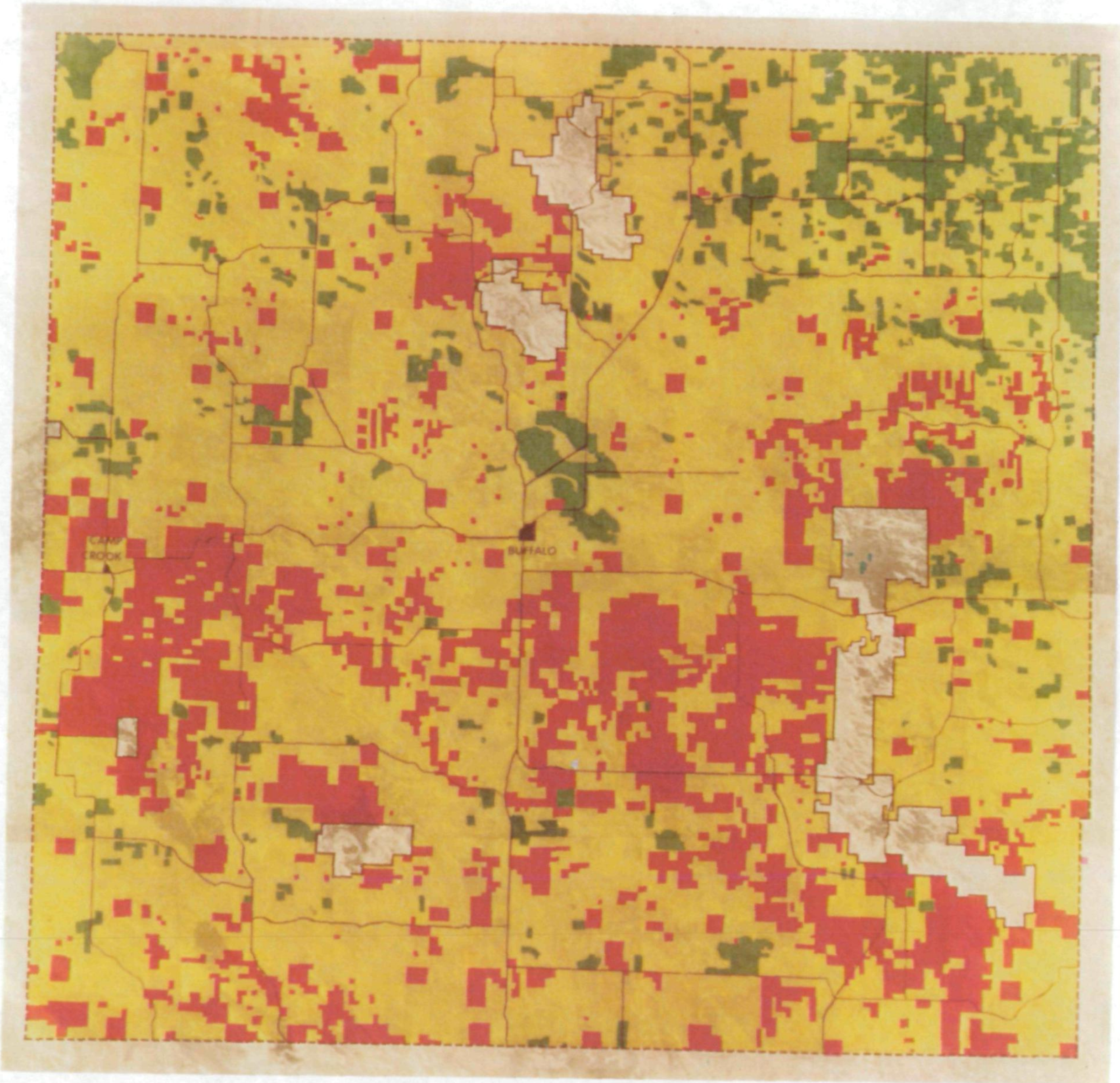

red - public rangeland
green - cultivated
yellow - private range land
clear - Custer National Forest

Figure 3. Map of sage grouse management potential for Harding County, South Dakota.

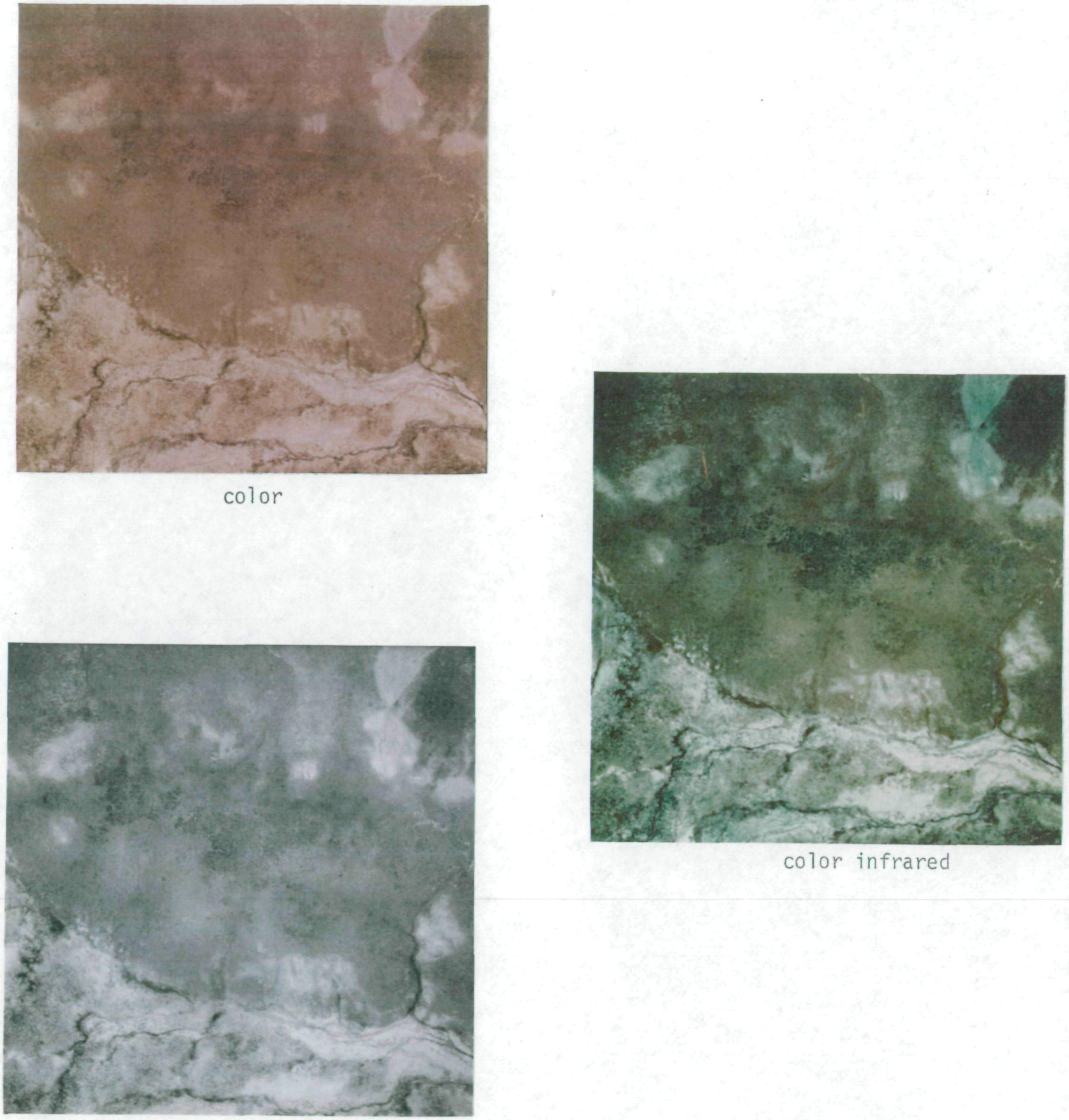

color

color infrared

black & white panchromatic

Figure 4. Large-scale (1:15,250) aerial photographs of transect 6 Butte County No. 3 study site collected 3 June 1981.

distinguishable on the larger scale photography. There were no apparent differences between the 2 species of sage brush on the photographs. Both Driscoll (1970) and Beck (1977) reported that sagebrush communities could be delineated on large scale aerial photographs. Driscoll (1970) reported a significant correlation between ground measurements of percent cover by big sagebrush and photo measurements of percent cover at scales of 1:500-1:1500. He concluded that several species, including sagebrush, had sufficient contrast with associated vegetation that they could be accurately delineated on aerial photographs collected any time during the growing season if the photo scales were large enough. Furthermore, he reported that the cost of measuring the vegetation along a transect on the ground was 10 times more expensive than making the measurements on aerial photographs.

The results of this project and those reported by other investigators indicate that sagebrush, the primary component of sage grouse habitat can be accurately delineated on large scale aerial photography collected any time during the growing season. The authors would recommend the use of color or black and white films for data collection during all times except "peak green" when color-infrared would be best. Sagebrush/grassland communities can be interpreted on small scale color-infrared imagery collected during "peak green".

Sage grouse are totally independent on sagebrush for food and cover during the winter (Patterson 1952, Eng and Schadweiler 1972, Wallestad et al. 1975). Eng and Schadweiler (1972) reported that sage grouse preferred sagebrush canopy coverage of 20% or more with an average of

28% for winter feeding and loafing. Beck (1977) found that density and height of sagebrush above snow cover as well as slope and aspect of the stand all have an effect on sage grouse winter use. Our field data suggest that while sufficient canopy cover is generally present the height of sagebrush above snow cover during normal winters may be a limiting factor because of short sagebrush found at the study sites.

The field data were substantiated with winter field observations and interpretations of Landsat imagery. Figures 5 and 6 are winter Landsat scenes of Butte County collected on 11 January 1980 and 17 February 1978, respectively. Snow depth for the county was 3 inches or less on 11 January 1980 and greater than 12 on 17 February 1978 (Figure 7). All grass and shrub vegetation was snow covered on 17 February 1978 resulting in the uniform light tones on the imagery. Most of the area had the same light tone on the Landsat imagery collected on 11 January 1980 when snow cover in the area was 3 inches or less.

One obvious difference is the dark tones evident in cultivated areas. The dark tones in cultivated areas probably result from standing crop residues that emerge through the snow cover. Sagebrush communities could not be distinguished on any of the Landsat winter scenes which would indicate that either they were snow covered or were not present at high enough density. The percent canopy coverage was greater than 50 percent in several areas and usually greater than 20 percent, both of which are probably greater than the coverage of the crop residues. This would indicate that the sagebrush, because of its short height, was snow covered even in periods of low snow depth. Figure 8 is a ground-level

Figure 5. Winter Landsat MSS 7 image of Butte County, South Dakota collected 11 January 1980. (ID 30677-16572).

Figure 6. Winter Landsat MSS 7 image of Butte County, South Dakota collected 17 February 1978. (ID 21122-16323).

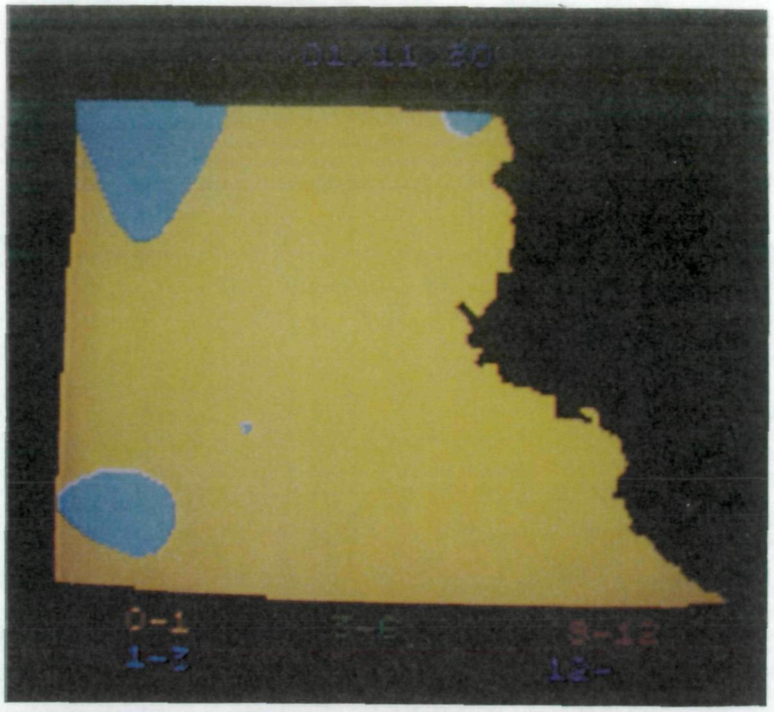

11 January 1980

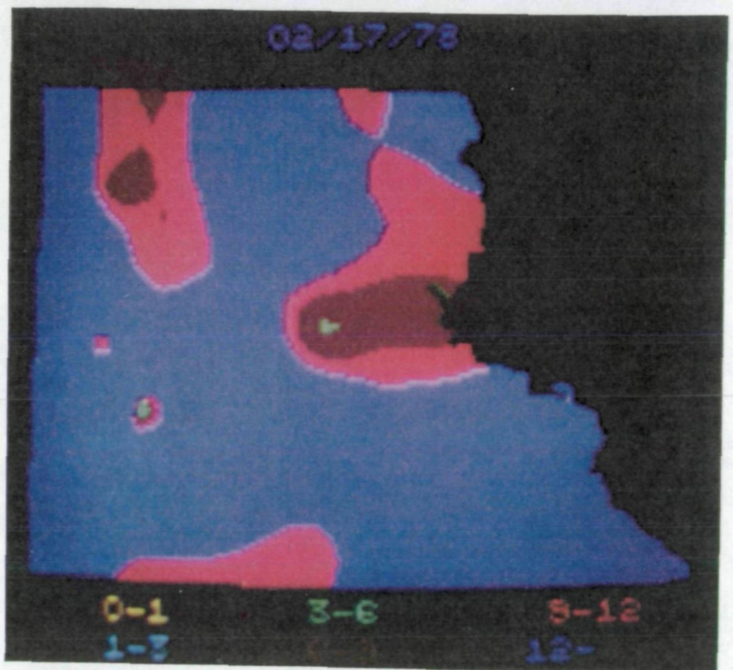

17 February 1978

Figure 7. Snow cover contour maps for 11 January 1980 and 17 February 1978.

Figure 8. Photograph of big sagebrush covered by drifting snow.

oblique photograph collected during the winter of 80-81 that illustrates the drifting snow which collects and may cover sagebrush communities. These data indicate the availability of suitable winter cover may be a serious limiting factor for sage grouse in South Dakota.

SUMMARY AND CONCLUSIONS

Interpretations of the sage grouse wintering and nesting habitat complex from remotely sensing imagery, used in conjunction with annual strutting ground counts, brood and hunter surveys provides a new perspective for sage grouse management in South Dakota. The results of this study indicate that in general the available habitat is suitable for nesting and brooding but may be too short to provide adequate winter habitat during periods of normal snowfall. It would be advantageous to sage grouse to limit the grazing of domestic livestock in areas where they utilize sagebrush for forage. A reduction in grazing may result in increased height of existing sagebrush which would improve winter habitat for the existing sage grouse populations. A general map showing potential areas for sage grouse management based on ownership and land use was prepared for Harding County, South Dakota.

The accuracy of photographic interpretation of sagebrush, the primary component of sage grouse habitat, depends on a combination of factors including the phenology of the sagebrush/grassland community, the film/filter combination used for data collection and the scale at which data are collected. Optimal aerial photography for interpretation

is color-infrared imagery collected during vegetative "peak green" at scales larger than 1:20,000.

LITERATURE CITED

Aldrich, J.W. 1963. Geographic orientation of American tetraonidae. J. Wildl. Manage. 27:529-545.

Batson, F.T. and J.C. Elliot. 1975. Surface resource inventory of eastern Montana rangelands utilizing high altitude color infrared aerial photography. Pages 117-128 in Proc. Fifth Biennial Workshop on Aerial Color Photography in Plant Sciences, EROS Data Center, Sioux Falls, SD.

Beck, D.I. 1977. Sage grouse flock characteristics on habitat selection in winter. J. Wildl. Manage. 41:18-26.

Best, R.G. and S. Sather-Blair. 1978. The interpretation of winter wildlife habitat in eastern South Dakota on Landsat imagery. Proc. Pecora IV Symposium on Application of Remote Sensing Data in Wildlife Management, Oct. 10-12, 1978 Sci. and Tech. Series No. 3. Natl. Wildl. Tech. pp.50-56.

__________ and K. Solomon. 1979. Interpretations of winter pheasant cover for the pheasant restoration program in South Dakota in Remote Sensing Application to Resource Problems in South Dakota. Annual Prog. Rpt. 1 July 1978 - 30 June 1979, pp.66-96.

Carnegie, D.M. 1968. Interpretation of color photography for range management in Smith, J.T., Jr. and A. Anson (Eds.). Manual of Color Aerial Photography, ASP, p. 408-409.

Daubenmire, R. 1959. A canopy-coverage method of vegetational analyses. Northwest Sci. 33:43-64.

Dougenik, J.A. and Sheehan, D.E. 1977. SYMAP users reference manual. Harvard University, Cambridge, Mass. 159pp.

Driscoll, R.S. 1970. Identification and measurement of shrub type vegetation on large-scale aerial photography. pages 32-1 to 32-15 in Third Annual Earth Resources Program Review, NASA Manned Spacecraft Center, Houston, Texas.

Driscoll, R.S., J.N. Reppert and R.C. Heller. 1974. Microdensitometry to identify plant communities and components of color infrared aerial photos. J. Range Manage. 27:66-70.

Eng, R.L. 1952. Population trends and breeding potential studies (sage grouse brood studies). Montana Fish and Game Comm., Wildl. Restoration Div. Quart. Prog. Rept. 3:56-62.

__________ and P. Schladweiler. 1972. Sage grouse winter movements and habitat use in central Montana. J. Wildl. Manage. 36:141-146.

Johnson, J.R. and J.R. Nichols. 1970. Plants of South Dakota grasslands: a photographic study. Bull. 566, Ag. Exp. Sta. SDSU. Brookings, SD, 163 pp.

June, J.W. Ed. 1969. Eighth western states sage grouse questionnaire. 200 pp.

Klebenow, D.A. 1969. Sage grouse nesting and brood habitat in Idaho. J. Wildl. Manage. 33:649-662.

__________ and G.M. Gray. 1968. Food habits of juvenile sage grouse. J. Range Manage. 21:81-83.

Patterson, R.L. 1952. The sage grouse in Wyoming. Wyoming Game and Fish Comm. Sage Books, Inc. Denver, Colorado. 341 pp.

Peterson, J.G. 1970. The food habits and summer distribution of juvenile sage grouse in central Montana. J. Wildl. Manage. 34:147-155.

Poulton, C.E. 1975. Range resources: inventory evaluation and monitoring in Reeves, R.G. (Ed.). Manual of Remote Sensing Vol. II, ASP, pp. 1427-1478.

Rasmussen, D.I., and L.A. Griner. 1938. Life history and management studies of the sage grouse in Utah, with special reference to nesting and feeding habits. Trans. N. Am. Wildl. Conf. 3:852-864.

Rogers, G.E. 1964. Sage grouse investigations in Colorado. Colorado Game, Fish and Parks Dept., Tech. Publ. 16. 132 pp.

Wallestad, R.O. 1971. Summer movements and habitat use by sage grouse broods in central Montana. J. Wildl. Manage. 35:129-136.

__________ and D. Pyrah. 1974. Movement and nesting of sage grouse hens in central Montana. J. Wildl. Manage. 38:630-633.

__________, J.G. Peterson and R.L. Eng. 1975. Foods of adult sage grouse in central Montana. J. Wildl. Manage. 39:628-630.

APPENDIX A

Summary of field data.

Site	Tran-sect	Canopy Cover (%) Big Sage	Canopy Cover (%) Silver Sage	Canopy Cover (%) Grass and Forbs	Canopy Cover (%) Bare Soil	Presence of Forbs (% of plots)	Density (Plants/40m²) Big Sage	Density (Plants/40m²) Silver Sage	Height (cm) Big Sage	Height (cm) Silver Sage	Crown Breadth (cm) Big Sage	Crown Breadth (cm) Silver Sage	Mean Cover (cm·Plants/40m²) Big Sage	Mean Cover (cm·Plants/40m²) Silver Sage	Distance From Lek (km)
Butte Co. No.1	1	14.1	0.0	17.3	60.1	0.0	117	--	12.1	--	25.5	--	1416	--	0.3
Butte Co. No.1	2	6.6	0.0	74.8	13.8	22.5	52	--	14.4	--	21.6	--	749	--	0.1
Butte Co. No.1	3	29.1	0.0	10.2	51.5	2.5	90	--	17.0	--	29.3	--	1522	--	0.9
Butte Co. No.1	4	17.9	0.0	64.9	9.3	0.0	33	--	16.0	--	32.6	--	528	--	1.8
Butte Co. No.1	5	21.0	0.0	46.5	23.4	0.0	49	--	21.0	--	35.6	--	1019	--	2.9
Butte Co. No.1	6	12.9	0.0	42.7	39.9	2.5	56	--	18.0	--	37.1	--	1008	--	2.3
Butte Co. No.2	1	22.9	0.0	13.2	57.1	0.0	166	--	8.1	--	20.4	--	1341	--	1.2
Butte Co. No.2 1/	2	0.0	19.3	49.0	23.6	0.0	--	52	--	29.3	--	40.0	--	1524	2.2
Butte Co. No.2	3	19.2	0.0	22.4	49.3	0.0	140	--	9.3	--	23.8	--	1302	--	3.2
Slim Buttes No.1	1	19.9	0.0	60.2	11.8	2.5	64	--	20.8	--	34.3	--	1321	--	0.5
Slim Buttes No.1	2	16.8	0.0	16.3	63.3	10.0	68	--	9.0	--	25.3	--	612	--	0.3
Slim Buttes No.1	3	20.9	3.2	69.8	3.1	87.5	22	7	35.7	37.2	62.9	39.0	785	242	0.6
Slim Buttes No.1	4	1.3	7.3	87.4	4.3	67.5	1	16	30.5	28.0	61.5	24.4	31	434	0.5
Slim Buttes No.1	5	7.6	0.0	90.0	7.9	47.5	10	--	20.4	--	32.3	--	204	--	0.5
Slim Buttes No.1	6	0.0	19.5	77.3	0.0	77.5	--	28	--	25.6	--	42.9	--	704	0.9
Slim Buttes No.1	7	0.0	16.7	82.9	0.0	77.5	--	57	--	25.7	--	28.8	--	1448	3.0
Slim Buttes No.1	8	15.9	0.0	52.1	22.0	10.0	49	--	16.0	--	30.9	--	776	--	2.0
Slim Buttes No.1	9	14.6	0.0	61.6	20.1	17.5	66	--	16.8	--	31.2	--	1100	--	1.4
Slim Buttes No.1	10	0.0	20.0	75.0	1.3	82.5	--	24.5	--	40.1	--	50.6	--	983	0.9
Slim Buttes No.1	11	15.1	0.0	57.8	19.4	50.0	42	--	21.1	--	32.0	--	856	--	1.7
Slim Buttes No.2	1	12.6	10.4	46.7	21.1	37.5	57	11	24.9	39.2	39.4	56.7	1407	412	0.5
Slim Buttes No.2	2	6.2	10.2	63.8	13.3	75.0	20	16	26.5	26.0	42.2	56.2	517	416	1.0
Slim Buttes No.2	3	0.0	15.1	82.6	1.6	52.5	--	41	--	30.0	--	41.5	--	1215	0.8
Slim Buttes No.2	4	7.3	14.8	75.0	1.3	67.5	7	18	27.9	27.4	51.9	42.6	181	480	0.5
Slim Buttes No.2	5	12.9	0.0	80.8	6.4	37.5	26	--	22.0	--	43.9	--	561	--	1.8

Site	Tran-sect	Canopy Cover (%) Big Sage	Canopy Cover (%) Silver Sage	Canopy Cover (%) Grass and Forbs	Canopy Cover (%) Bare Soil	Presence of Forbs (% of plots)	Density (Plants/40m²) Big Sage	Density (Plants/40m²) Silver Sage	Height (cm) Big Sage	Height (cm) Silver Sage	Crown Breadth (cm) Big Sage	Crown Breadth (cm) Silver Sage	Mean Cover (cm·Plants/40m²) Big Sage	Mean Cover (cm·Plants/40m²) Silver Sage	Distance From Lek (km)
Slim Buttes No.2	6	5.2	4.6	91.0	0.0	82.5	7	9	30.5	22.5	45.0	38.6	198	202	1.1
Slim Buttes No.2	7	10.7	0.0	61.1	24.5	82.5	36	--	24.4	--	37.8	--	866	--	0.8
Slim Buttes No.2	8	13.3	0.0	70.4	11.4	42.5	48	--	17.8	--	30.5	--	846	--	2.1
Mallula Area2/	1	58.7	0.0	47.1	0.0	69.8	44	--	52.7	--	56.6	--	2293	--	4/
Mallula Area2/	2	40.6	0.0	34.1	20.8	47.5	89	--	25.5	--	33.8	--	2257	--	4/
Little Missouri	1	19.0	0.0	69.8	5.9	48.0	31	--	33.3	--	48.5	--	1016	--	4/
West Short Pines	1	22.1	0.0	70.0	3.2	70.0	32	--	28.7	--	49.5	--	918	--	4/
Butte Co. No.3	1	23.8	0.0	61.0	9.8	57.5	43	--	31.9	--	44.4	--	1372	--	0.1
Butte Co. No.3	2	37.6	0.0	40.4	18.0	47.5	67	--	34.0	--	51.8	--	2261	--	0.5
Butte Co. No.31/	3	24.5	13.7	29.7	26.1	7.5	40	14	30.3	35.5	39.3	43.3	1197	497	1.5
Butte Co. No.31/	4	0.0	35.4	59.9	4.3	67.5	--	57	--	42.8	--	49.9	--	2440	1.8
Butte Co. No.3	5	14.9	0.0	78.7	5.2	75.0	33	--	27.6	--	36.2	--	597	--	0.6
Butte Co. No.3	6	54.1	0.0	29.2	11.6	20.0	55	--	42.6	--	54.4	--	2322	--	1.0
Butte Co. No.3	7	14.4	0.0	33.5	44.1	47.5	41	--	20.2	--	32.5	--	818	--	1.6
Butte Co. No.3	8	18.9	0.0	52.7	23.4	37.5	44	--	23.9	--	32.2	--	1052	--	1.1
Butte Co. No.4	1	30.2	0.0	31.0	31.4	70.0	74	--	26.8	--	43.4	--	1983	--	0.6
Butte Co. No.4	2	18.3	0.0	33.8	39.8	60.0	53	--	19.8	--	30.6	--	1040	--	1.0
Butte Co. No.4	3	17.9	0.0	59.5	16.2	37.5	35	--	22.6	--	39.7	--	791	--	0.8
Butte Co. No.4	4	12.4	0.0	6.1	79.4	2.5	51	--	20.8	--	33.4	--	1061	--	0.2
Butte Co. No.41/	5	12.1	14.4	49.4	22.5	37.5	14	32	42.6	44.1	49.8	49.9	575	1411	1.4
Butte Co. No.43/	6	7.9	0.0	62.1	18.6	62.5	13	--	26.7	--	46.5	--	347	--	2.3

1/Creek bottoms

2/Transects 1 and 2 had 19.7 and 8.6% canopy cover of dead sage respectively

3/Creek bottom with 9.8% canopy cover of greasewood

4/Location of lek unknown; evidence of sage grouse usage present

COMPUTERIZED DIGITIZATION OF AERIAL THERMAL INFRARED DATA FOR CENSUSING CANADA GEESE

By

R.G. Best, R. Fowler, D. Hause and M. Wehde

ABSTRACT

The use of aerial thermal infrared imagery for censusing Canada geese has been demonstrated in a previous project. The production of thermal infrared imagery from the recorded scanner signal may introduce system limitations which reduce the apparent quality and resolution of the data. Limitations in film recording from the analog signal could adversely affect evaluation of thermal infrared detection capabilities for small targets. The objective of this project was to evaluate computerized digitization of the original analog aerial thermal infrared signal for delineating Canada geese. The Signal Analysis and Dissemination Equipment (SADE) at RSI was modified for analog-to-digital conversion at several cross-track sampling rates from 190 to 10,500 samples per scan line. Digitization rates of 350, 1350 and 2670 samples per scan line were evaluated for delineating low densities of geese in widely dispersed flocks and for delineating density differences within high density flocks.

COMPUTERIZED DIGITIZATION OF AERIAL THERMAL INFRARED DATA FOR CENSUSING CANADA GEESE

By

R.G. Best, R. Fowler, D. Hause and M. Wehde

INTRODUCTION

This project was a follow-on to the NASA project entitled "Thermal Infrared Census of Canada Geese in South Dakota" (Best and Fowler 1980a, 1980b). Radiant heat loss measurements from Canada geese indicated that sufficient apparent temperature contrast should be present to distinguish Canada geese resting in open water on aerial thermal infrared data (Best and Fowler 1980). Results of that project indicated that it was feasible to use aerial thermography in an operational technique for Canada goose census with some limitations. Goose concentrations could be detected on the aerial thermography collected in that project at altitudes less than 1500 feet above ground level (AGL). Groups as small as two geese in close proximity to one another can be interpreted on thermal imagery collected at 1,000 ft. AGL. The methodology developed in that project was to estimate the total number of geese from the product of the area of geese measured on aerial thermography and an empirical goose density derived from counts on aerial photos and ground truth. This technique will provide an estimate but not a count.

The production of imagery with the Cathode Ray Tube (CRT) system may be limiting the information content of the imagery as a result of data smoothing during image generation. The thermal information

interpretable by direct computerized digititation of the analog thermal signal should surpass the visual representations generated on CRT produced images and may make counts of individual geese possible.

Goldsbrough (1977) concluded that there was a considerable improvement in thermal detail when contour plots were generated from digitized thermal scanner data. He reported an improvement in signal-to-noise ratio when an exponential smoothing technique was used.

The objective of this project was to evaluate computerized digitization of aerial thermal infrared data to improve the delineation of Canada geese. The technique was evaluated under two conditions: (1) low concentrations of widely dispersed geese; and (2) heavy concentrations of geese. In the first case the technique was tested to determine if single geese can be distinguished from the background. In the second case it was necessary to determine if individual geese can be distinguished from the background and from other geese which are in close proximity. This approach should facilitate a better assessment of the utility of aerial thermal infrared data in census applications involving small dispersed targets.

PROCEDURES

Aerial thermal infrared scanner tape recordings collected over goose concentrations on the Missouri River Reservoir during the fall and winter of 1979-80 were converted to digital image matrices for computer processing. Thermal data with both high densities of geese on an ice and

open water background and low densities of widely dispersed geese were selected to evaluate the digitization process.

The Signal Analysis and Dissemination Equipment (SADE) system analog-to-digital conversion hardware and software was modified to accommodate a wider sampling range through time scaled playback and engineering changes. The system was redesigned to produce crosstrack sampling rates of 190, 350, 1350, 2670 and 10,500 samples per scan line. The five digitization rates are determined by the playback speed of the analog tape deck. The analog tape deck has three speeds for reproducing the recorded scanner signal: 30 inches per second (ips); 15 ips and 3 3/4 ips. Using two compatible tape decks, one to reproduce the original signal at 3 3/4 ips and re-record at 30 ips provides five playback rates for digitization.

An Ohio Scientific Microprocessor System was interfaced to command/control the conversion process. Data sample-and-store software were implemented to build a digital image file during the conversion process. High spatial resolution digitization of experimental study areas yielded matrices of image data which were directly accessed, searched, isolated, enhanced and displayed with existing software designed to utilize the disk file.

The aerial thermal infrared data were digitized at 3 rates, 350, 1350 and 2670 samples per scan line, in this project. The lowest sampling rate generates pixels that represent ground intervals approximately 2X the instantaneous-field-of-view (IFOV) of the original data. The 1350 and 2670 digitization rates generate pixels that represent ground intervals approximately equal to 1/2 and 1/4 the IFOV of the original data, respectively.

A small subarea in the digital matrix that coincides with the center of a single aerial photograph was selected for display. The spatial arrangement of geese at the instant recorded by the photography only corresponds to slightly more than one scan line. Additional scan lines recorded between photographic frames will image spatial relationships as they change. Thus the selection of a digital image subarea from the thermal data which is in close proximity to a photo frame center assures that the spatial relationships within the photo are as close as possible to those actually recorded by the scanner. The digital data were color encoded into 8 equal intervals and displayed on color CRT. Software was utilized to improve the observation of temperature resolution by contrast stretching digital values.

RESULTS AND DISCUSSION

The original thermal infrared radiance data are recorded as an analog signal. The radiance value at any point in the analog data is determined by the proportion of each target and the magnitude of the apparent temperature of each target within the IFOV. It may be possible to detect the presence of a target smaller than the IFOV if the apparent temperature difference between the target and background feature is large enough. It is not possible to detect the precise location; only that the target is within that IFOV.

The cross-track resolution of the original analog data is a function of the scanner and detector viewing geometry and the altitude of data collection. The smallest IFOV is at the nadir and the largest is at the

maximum look angle. The IFOV is 2.5 ft. at the nadir and 4.8 ft. at the maximum look angle when data are collected at an altitude of 1000 ft. with the 2.5 milliradian detector and Daedalus thermal scanner system used in this project.

The effective ground spacing of cross-track IFOVs in the digital data is determined by the sampling rate and the altitude of the data collection. Table 1 is a summary of cross-track ground sampling increments at two altitudes.

Table 1. Cross-track ground sampling increment at various sampling rates and altitudes.

Sampling Rate Samples/Scan Line	Ground Sampling Increment (ft.) 1000 ft. AGL	1500 ft. AGL
190	8.42	12.63
350	4.57	6.86
1350	1.18	1.78
2670	0.59	0.90
10500	0.15	0.23

The along-track coverage and resolution is a function of aircraft speed, altitude and scanner characteristics and is not changed by digitization. The effective along-track resolution of the system used is approximately 2.5 ft. when data are collected at an altitude of 1000 ft. AGL.

Subtle tonal differences related to small apparent temperature differences are difficult to detect on continuous tone analog aerial thermal infrared imagery (thermography). Visual interpretations of geese

on thermography can be very subjective if the apparent temperature of geese is close to that of the open water or snow and ice background. Interpretations are further complicated when geese are present in low numbers in widely dispersed flocks (Figure 1).

Digitization assigns a discrete value, relative to the thermal radiance, to each picture element (pixel). Pixels can be color encoded in up to 16 equal apparent temperature increments and displayed on the SADE monitor (Figure 2). The small sub-area, outlined by a rectangle, was selected for displaying and evaluating digitization rates. The data matrix for the sub area is small enough to display on one screen, even at high digitization rates. The aerial thermal infrared data were digitized at 3 cross-track sampling rates; 350, 1350 and 2670 samples per scan line (Figure 3). Pixels in which geese are present have the highest digital values. Scan line traces were used to determine a threshold value that would include only pixels in which geese are present (Figure 4). Distance along the X axis of the graphs is relative to position along the scan line. Pixels with a digital value greater than 224 were assigned a yellow color and probably represent samples in which geese are present. The exact digital value threshold selected to isolate geese is dependent on environmental conditions and scanner setup.

The lowest sampling rate generates pixels that represent ground intervals approximately 2x the size of the IFOV of the original data. The probability of detecting a single goose or small groups of geese decreases when the sampling interval is greater than the IFOV. These data are suitable for previewing and determining the location of geese.

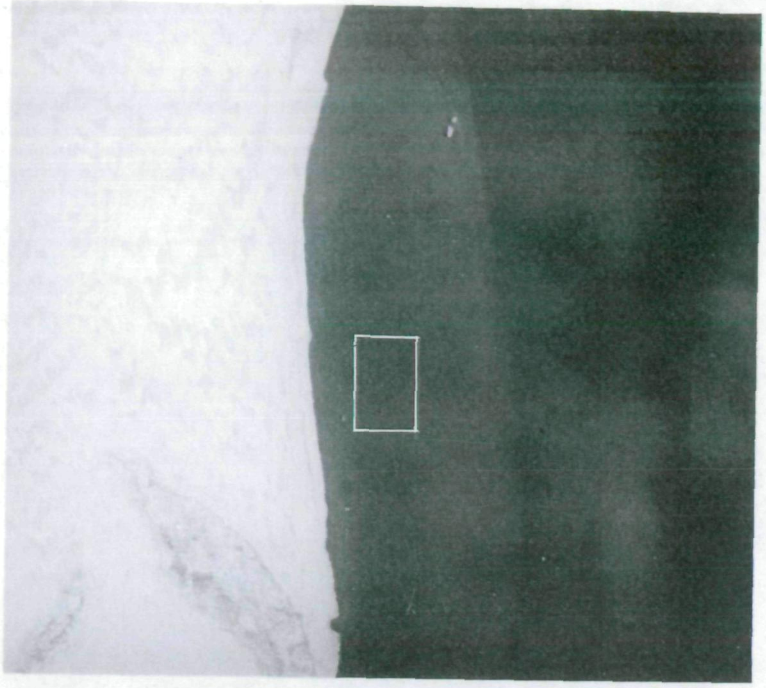

aerial photograph

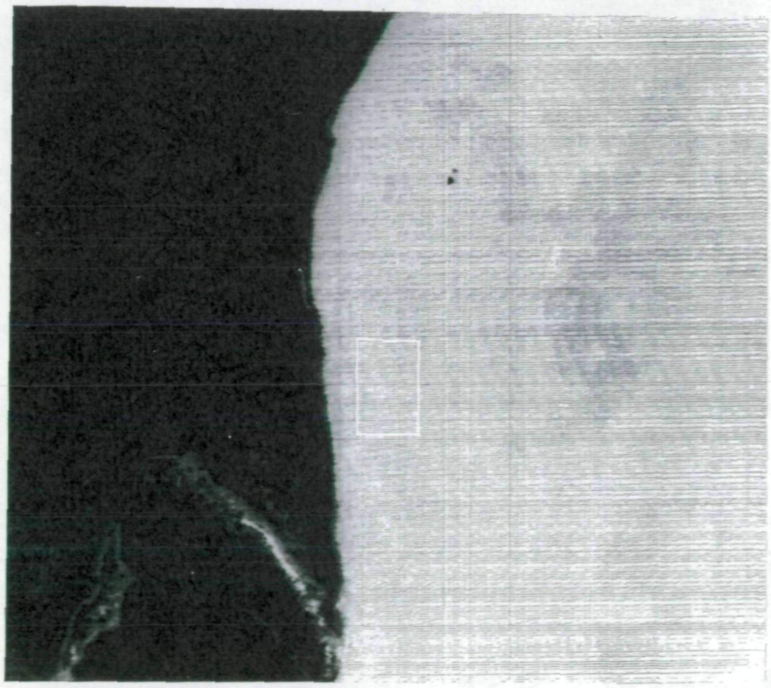

thermal infrared image

Figure 1. Aerial photograph and analog thermal infrared image of low density widely dispersed flock of Canada geese. The area enclosed by rectangle was selected for display at 3 different digitization rates.

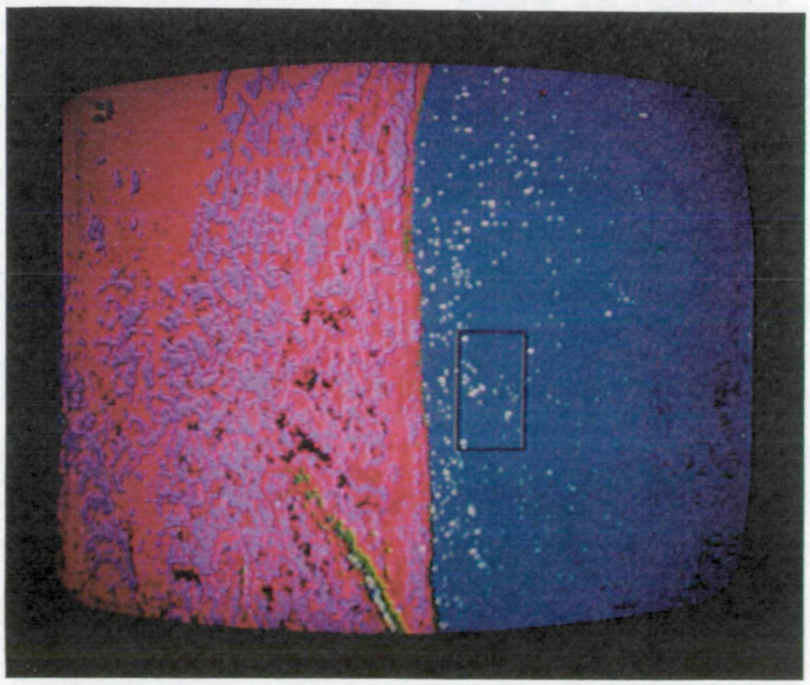

Figure 2. Display of digital data coinciding with aerial photograph and thermal infrared image in Figure 1. The area enclosed by the rectangle was selected for display at 3 digitization rates in Figure 3.

350 samples/scan line

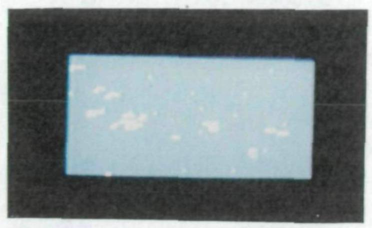

1350 samples scan line

2670 sample/scan line

Figure 3. Displays of subarea enclosed by rectangle in Figure 2 at digitization rates of 350, 1350 and 2670 samples/scan line.

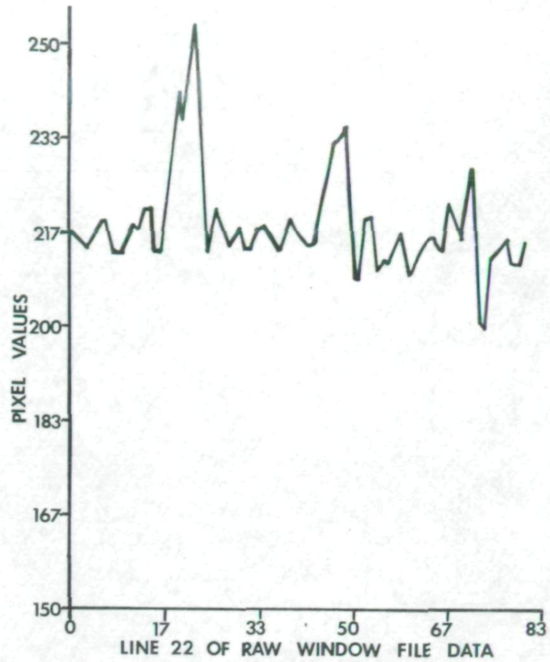

1350 samples/scan line

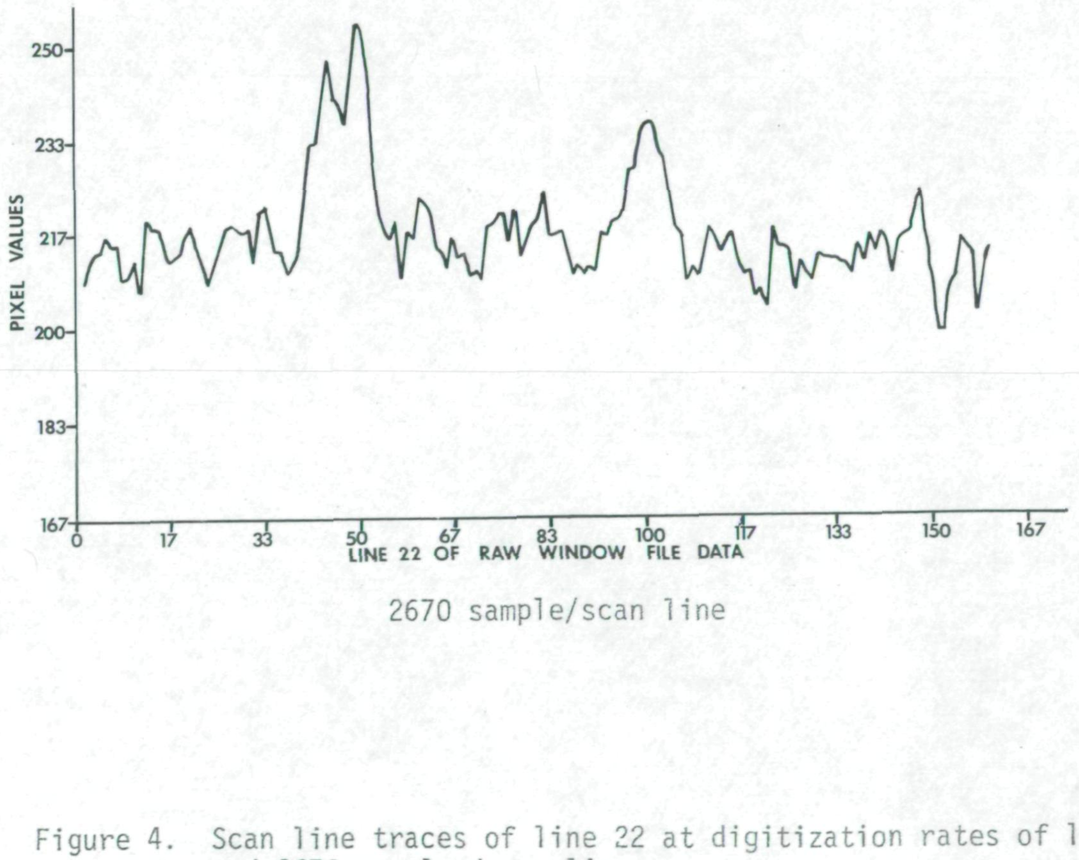

2670 sample/scan line

Figure 4. Scan line traces of line 22 at digitization rates of 1350 and 2670 samples/scan line.

The 2 higher digitization rates generate pixels that represent ground intervals smaller than the IFOV of the original data. The cross-track dimension increases proportionally with the digitization rate which results in cross-track spatial distortion of the data. The aspect can be corrected during processing by duplicating scan lines. An increase in the digitization rate increases the probability of detecting a goose by increasing the probability of sampling a peak in the original analog data. Furthermore, there is a potential for more pixels per goose at higher digitization rates. It was possible to identify pixels that may be small groups or individual geese at the higher digitization rates but it was not possible to distinguish individual geese that were in close proximity.

When geese occur in large dense flocks, it is not difficult to interpret the location or aerial extent of the flocks on thermography (Figure 5). However, subjectivity in delineating areas of different densities of geese within the flock may result in errors when estimating total numbers. Digitization and thresholding can be used to isolate thermal anomalies related to differences in goose density (Figures 6 and 7). The thermal patterns of the high density goose flocks were similar at the 3 digitization rates tested in this project (Figure 7). The colors within the flock on digital display reflect differences in apparent temperature that may be a result of goose density differences. The SADE system has a built-in planimeter which may be used to measure the area of any one or more color levels. The midrange digitization rate (1350 sample per scan line) would probably provide the best results. At this digitization rate, the ground interval represented by a pixel is smaller than the IFOV

aerial photograph

thermal infrared image

Figure 5. Aerial photograph and thermal infrared image of high density goose flock resting on water and snow and ice background.

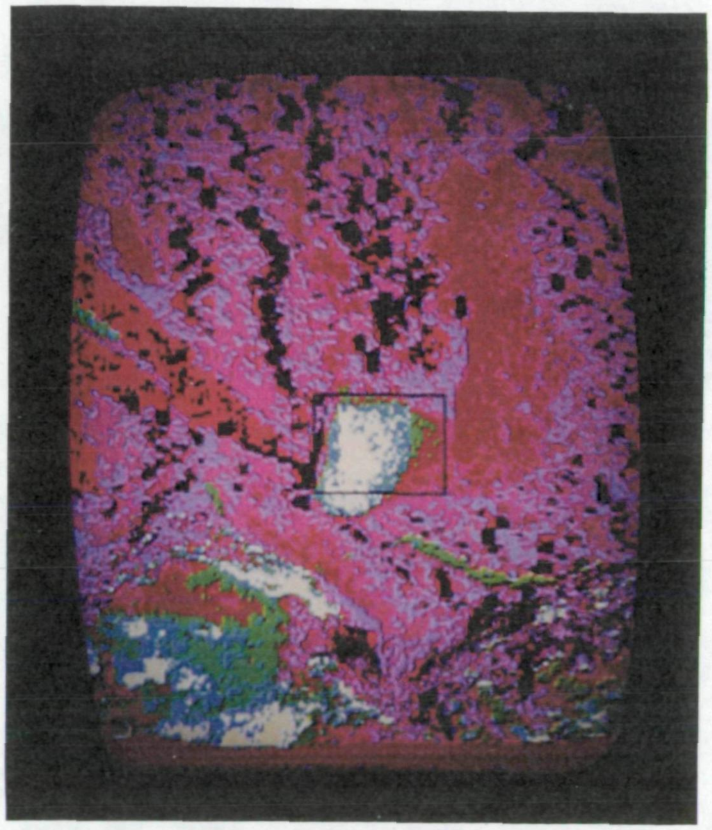

Figure 6. Display of digital data coinciding with aerial photograph and thermal infrared image in Figure 5. The area enclosed by the rectangle was selected for display at 3 digitization rates in Figure 7.

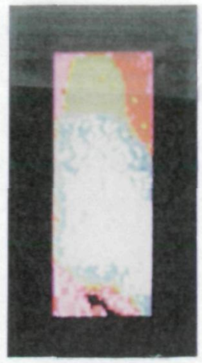

350 samples/scan line

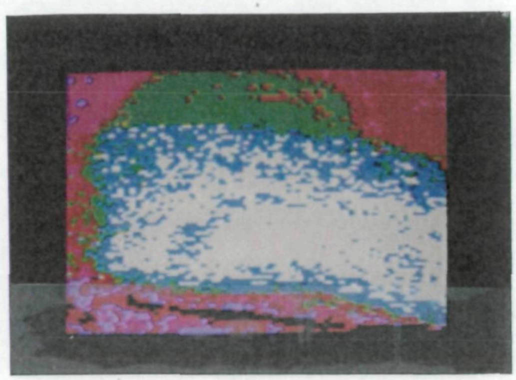

1350 samples/scan line

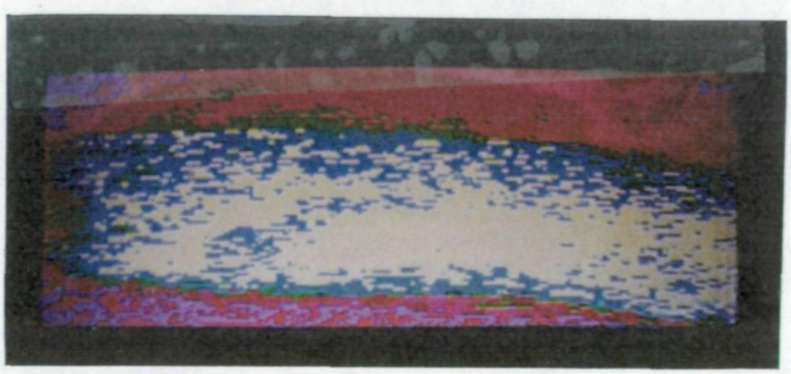

2670 samples/scan line

Figure 7. Displays of subarea enclosed by rectangle in Figure 6 at digitization rates of 350, 1350 and 2670 samples/scan line.

of the original data and the data matrix is smaller and more manageable than at higher digitization rates.

Contrast stretch options available on the SADE system can be employed to enhance apparent temperature differences in the digital displays. Contrast options can also be used to refine the thresholding of the digital matrix. There is a potential for improving the spatial resolution of aerial thermal infrared data if a proportion estimation algorithm can be developed to calculate digital pixel values based on the overlapping IFOVs of the original analog data and the digitization rate. It is possible to develop software to improve the signal-to-noise ratio using the over-sampling of the higher digitization rates to average out certain noise components.

SUMMARY AND CONCLUSIONS

The visual interpretation of Canada geese on aerial thermal infrared imagery can be very subjective because of their small size and lack of apparent temperature contrast under certain environmental conditions. The delineation of the thermal infrared signature of geese on open water or snow and ice background requires intense sampling rates compatible with the target size at the altitudes involved, signal frequency fidelity and recording media playback rates. The computerized digital analysis of the aerial thermal infrared analog signal can generate sampling rates that represent ground increments smaller than the IFOV of the scanner system. It may be possible to improve the spatial resolution of aerial thermal

infrared data if a proportion estimation algorithm can be developed to calculate digital pixel values based on the overlapping IFOVs of the original analog signal and the digitization rate. Thresholding and contrast stretch options can be used to enhance apparent temperature differences and reduce interpretation subjectivity.

There is information present in the analog signal that is not interpretable on thermography which may be developed with proper processing techniques into an improved source of thermal infrared information.

LITERATURE CITED

Best, R.G. and R. Fowler. 1980a. Thermal infrared census of Canada geese in South Dakota. Pages 21-53 in V.I. Meyers P.I., Remote Sensing Applications to Resource Problems in South Dakota. Semi-annual Progress Report, 1 July 1979 - 31 December 1979. SDSU-RSI-80-02.

_________ and _________. 1980b. Thermal infrared census of Canada geese in South Dakota. Pages 28-52 in V.I. Myers P.I., Remote Sensing Applications to Resource Problems in South Dakota. Annual Progress Report, 1 July 1979 - 30 June 1980. SDSU-RSI-80-06.

_________ and _________. 1981. Infrared emissivity and radiant surface temperatures of Canada and snow geese. (Accepted for publication) J. Wildl. Manage.

Goldsbrough, P.F. 1977. Digital processing of analog thermal infrared scanner data. Photogrametric Engineering and Remote Sensing 43(2) 145-153.

UTILIZATION OF LANDSAT DATA FOR MONITORING GRASSHOPPER INFESTATION IN RANGELAND

By

R. G. Best and K. Winks

ABSTRACT

Infestations of grasshoppers can greatly reduce the productivity and lower the livestock carrying capacity of western rangelands. Current methods for monitoring grasshoppers require extensive manpower and are extremely costly. The objective of this project was to evaluate the use of Landsat data for delineating infested areas by monitoring their effect on rangeland biomass. Data on distribution and abundance of grasshoppers were collected using current field methods and maps were produced with a computerized mapping system (SYMAP). Manual interpretation of Landsat RBV and MSS imagery were evaluated for Corson County in north central South Dakota. Subtle tonal differences, which may correlate with grasshopper infestations, were evident on MSS imagery but no accurate delineation could be made. No patterns associated with grasshopper infestations could be detected on the Kauth-Thomas or band ratio index transformations tested in this project. A principal component analysis may be necessary to isolate a vegetative component that would correlate with grasshopper density.

UTILIZATION OF LANDSAT DATA FOR MONITORING GRASSHOPPER INFESTATION IN RANGELAND

By

R. G. Best and K. Winks[1/]

INTRODUCTION

Grasshoppers are found throughout the United States and are the principal invertebrate consumers of forage on approximately 665 million acres of rangeland in the western United States (Hewitt et al. 1976). Severe infestations occur most frequently in the Northern Great Plains including eastern Montana, North Dakota, South Dakota, Nebraska and Kansas (Parker, 1952). Surveys made in the fall of 1979 indicate that 32,194,634 acres of rangeland were infested with grasshoppers and had the potential for severe grasshopper infestations in 1980. These figures represent only areas with more than 8 grasshoppers per square yard. Control at this density level is economically practical. Regions with a density of 3 to 7 grasshoppers per square yard could also become problem areas if it is dry during hatching in May and June. Control of grasshoppers at this density level is not usually economically practical, even though there may be extensive damage to range grasses. These surveys indicate that 1,768,610 acres of rangeland in western South Dakota were infested with more than 8 grasshoppers per square yard in 1979. Climatic

[1/] Remote Sensing Institute, South Dakota State University, Brookings, South Dakota 57007, and Animal and Plant Health Inspection Service, USDA, Federal Building, Bismarck, North Dakota 58501, respectively.

and biotic conditions during the spring determine the exact areas affected in 1980.

High concentrations of grasshoppers can greatly reduce the productivity of rangeland and lower the livestock carrying capacity. Infestations of 20 to 50 per square yard have frequently destroyed 75 to 100 percent of available forage by midsummer during drought years (Parker, 1952). Morton (1936) found an average loss of 67.0% of the total range production during the summer of 1936. He reported losses as high as 97.3% in some areas. Parker (1952) reports that the lesser migratory grasshopper eats 24 milligrams per day. At a density of 31 per square yard over 2 acres, the grasshoppers would eat an amount of forage equivalent to that eaten by a cow/day. A concentration of 7 grasshoppers per square yard on 1 acre will eat about 1/10 as much forage as a cow.

The U. S. Department of Agriculture (USDA) Animal and Plant Health Inspection Service (APHIS) has the responsibility of determining the distribution of grasshopper infestations and, in conjunction with the state extension service entomologist, suggesting control procedures. The data obtained in the surveys are essential to federal, state and county officials, industry and growers in order to prepare for situations which might develop into costly emergencies. The current technique for determining potential grasshopper infestations is a ground survey during summer and fall. The surveys require extensive manpower and are very costly because of the large areas involved. A reconnaissance technique based on Landsat data would greatly reduce the costs of the annual survey.

Hielkema and Howard (1976) attempted to locate breeding areas of locust in a desert landscape with remotely sensed data by locating areas of lush vegetation. The interpretations were relatively simple because vegetated areas were the only suitable locust habitat and they contrasted with desert areas.

This project did not attempt to enumerate grasshoppers, but was designed to identify infestations by their effect on rangeland biomass. Investigators have studied the use of remote sensing for monitoring changes in biomass in a grassland biome (Pearson and Miller, 1972; Tucker et al. 1975). These studies are based on radiometer and airborne multispectral scanner data, but Pearson and Miller (1972) concluded that the techniques would be applicable for satellite borne sensor data. Poulton (1975) illustrates the use of Landsat color composites for monitoring rangeland forage. Carneggie and De Gloria (1972) discussed the use of Landsat data for determining range condition and estimating forage production. Maxwell (1976) used a statistical analysis of digital Landsat data in order to classify standing crop biomass for selected species and range types. The signature of a crop or rangeland was influenced by three discrete components: 1) soil (including shadow); 2) non-growing vegetation; and 3) growing vegetation. Research has indicated a good potential for digital analysis of Landsat data for distinguishing vegetative biomass and condition. Vegetation index models have been designed, in part, to reduce the effects of soils and other background on the signature of the vegetation.

The objectives of this project are: 1) to evaluate manual interpretation of Landsat imagery for monitoring grasshopper infestations in rangeland; and 2) to evaluate the use of digital analysis of Landsat data for monitoring grasshopper infestations in rangeland.

PROCEDURES

Rangeland biomass studies have generally been quantitative requiring extensive ground level biomass sampling. This study was more qualitative in an attempt to compare infested vs. noninfested areas. The assumption was that infested areas would have reduced biomass proportional to the grasshopper density.

Grasshopper density data for western South Dakota were collected by USDA/APHIS personnel following procedures described in the USDA publication entitled "Grasshopper Survey". An estimate of the number of adult grasshoppers is made by counting the number of grasshoppers leaving a square-yard area or extrapolating numbers from square-foot samples. The number of grasshoppers per square yard is recorded at sample location on county road maps. Twenty-five to 50 stops are made in each county depending on the nature of the infestation, supervisor's knowledge of infestation and size of county. The grasshopper density data were encoded into a computerized spatial storage and retrieval system (SYMAP) developed at Harvard University (Dougenik and Sheehan, 1977). The outputs from the system were computerized symbol overstrike contour maps and color displays produced via RSI's Signal Analysis and Dissemination Equipment (SADE) system. Corson County in northcentral South Dakota

was selected as the study site by RSI, APHIS and SDSU extension personnel. Spring and summer (1980) Landsat data of Corson County were acquired from the EROS Data Center for analysis (Table 1). Standard and contrast enhanced false color-infrared composites of MSS 4, 5, and 7 were prepared at RSI.

Table 1. Landsat data for Corson County, South Dakota acquired for grasshopper density analysis.

Date	Scene I.D.	MSS 4	MSS 5	MSS 7	Color Composite	RBV	CCT
9 April 1980	30766-16484-D					X	
15 May 1980	30802-16480-D					X	
2 June 1980	30820-16473-D					X	
29 June 1980	21985-16532	X	X	X	X		
22 Aug. 1980	22039-16541	X	X	X	X		X
9 Sept. 1980	22057-16541	X	X	X	X*		X

*Photographically enhanced composite produced in addition to standard composite.

Tone, texture, and patterns were the criteria used for image interpretation. Tone is the lightness or darkness on a photographic image and corresponds to the reflectance at a particular site. The frequency of tonal changes which appear as a continuum from smooth to rough appearances on an image is photographic texture. Pattern can be defined as image features at a given scale which can be identified by regularity and placements of tones and texture.

Transformations of digital Landsat data (CCT's), that have proven successful for other investigators, were generated for 22 August 1980 and 9 September 1980. The Kauth-Thomas (1976) transformation partitions the 4 band MSS data into 4 components, soil brightness index (SBI), green vegetation index (GVI), yellow matter index (YMI), and "non-such" (NS). Kauth and Thomas (1976) use the following coefficients in their transformation models:

$$SBI = 0.433MSS4 + 0.632MSS5 + 0.586MSS6 + 0.264MSS7$$

$$GVI = -0.290MSS4 - 0.562MSS5 + 0.600MSS6 + 0.491MSS7$$

$$YMI = -0.829MSS4 + 0.522MSS5 - 0.039MSS6 + 0.194MSS7$$

$$NS = 0.223MSS4 + 0.012MSS5 - 0.543MSS6 + 0.810MSS7$$

The second transformation used was a modification of the transformed vegetation index (TVI) developed by Deering et al. (1975) and described by Harlan et al. (1979). The form used in this project was a normalized difference index (ND) in the form:

$$ND\ 6 = (MSS6 - MSS5)/(MSS6 + MSS5)$$

The MSS6 + MSS5 term acts as a normalizing term and the data were scaled from 1 to 255 which was compatible with image generation equipment. One percent of the data were truncated and the data were linearly stretched prior to the image generation. All possible 2 band ratio indexes were prepared from 9 September 1980 as a supplement to the other 2 proven indexes.

RESULTS AND DISCUSSION

Corson County was selected as the study site because of the close proximity of infested and noninfested areas and a similarity in soil and vegetation associations. Figure 1 is a SYMAP display of the abundance and distribution of grasshoppers in Corson County. This area was also selected because growing season rainfall was nearly normal in the county while much of western South Dakota was experiencing a severe drought. Drought in many parts of western South Dakota was so severe that it provided natural grasshopper control and prevented expansion of infestations. Corson County did experience very dry conditions early in the growing season which delayed spring green up. Normal and above normal rainfall occurred in the area late in the growing season.

Subtle tonal differences which may correlate with grasshopper infestations were most evident on MSS4 imagery collected on 29 June 1980. These data represent green spectral reflectance. The darkest tones indicating the lowest relative green reflectance were evident in the infested areas. No tonal variations were evident between the severe and threatening infestations but differences between infested and noninfested areas could be detected. Although there appears to be tonal difference between infested and noninfested areas, accurate delineations of the areas could not be visually interpreted on imagery. Subtle reflectance difference between infested and noninfested areas were also present on other MSS bands and on other dates. The difference may be a result of low vegetation density caused by a lack of precipitation and overgrazing by domestic livestock. Atmospheric attenuation, soil

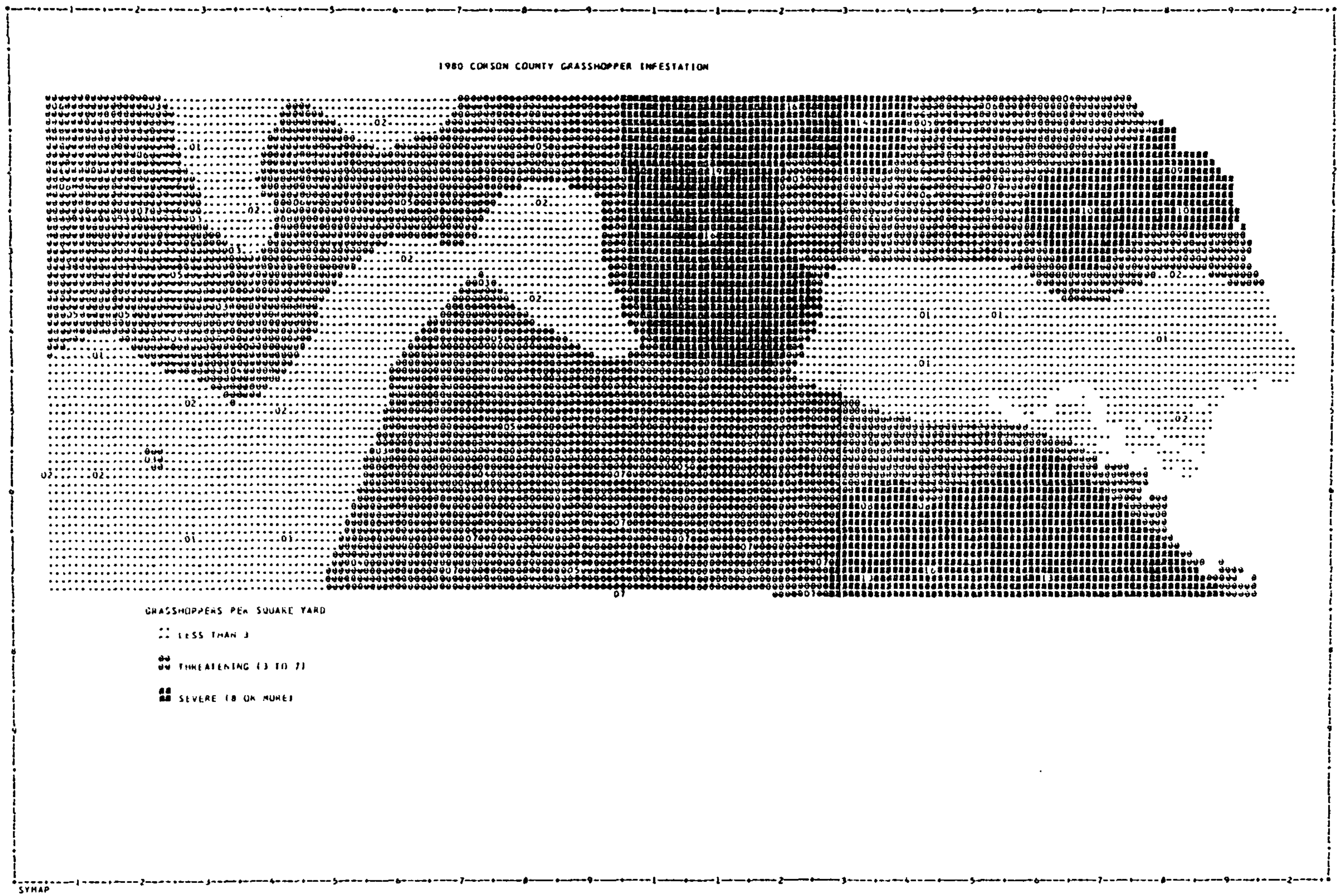

Figure 1. SYMAP display of 1980 grasshopper infestation for Corson County, South Dakota, prepared from field data.

type, soil moisture, land use practices and photographic processing techniques may also have affected the apparent tonal differences on the MSS imagery.

Only one of the RBV scenes acquired for this project was collected late enough in the season to show the effects of high populations of grasshoppers. No apparent spectral differences were obvious on the RBV imagery. These data are collected over a broader spectral range with an increased spatial resolution. The improved spatial resolution of the RBV imagery did not, however, enhance spectral differences related to infested areas.

Several investigators have attempted to distinguish the soil components from the vegetation components. Kauth and Thomas (1976) developed a linear preprocessing transformation of Landsat digital data which isolated growing and non-growing vegetation and soil brightness in the midwestern U. S. corn belt. They followed the progression of crops from bare soil to full canopy on Landsat data. By utilizing all four Landsat bands, a temporal pattern emerged which was labelled the "tasselled cap"; its formative elements were determined by the following indices: 1) in the early part of the season the soil dominates the recorded reflectance; 2) as growing vegetation covers the soil, increased reflectance takes place in the near-IR (Landsat bands 6 and 7) while increased absorption takes place in bands 4 and 5; 3) when a full canopy masks the soil and the influence of soil color is effectively eliminated; and 4) when the crop matures or yellows and reflectance changes accordingly.

The Kauth-Thomas transformations for Corson County, generated from 9 September 1980 Landsat data are presented in Figures 2-4. Differences are present among cultivated fields and between cultivated areas and rangeland on the GVI transformation (Figure 2). Differences within the rangeland do not appear to be associated with a reduced biomass resulting from grasshopper infestations. Patterns on the SBI (Figure 3) did not correlate with mapped soil associations. Furthermore, the SBI for both dates were dissimilar which indicate that the Kauth-Thomas transformations are not defining the soil component in the study area. The YMI (Figure 4) did not provide any additional useful information for delineating areas of grasshopper infestation. The numerous image features that can be distinguished on the non-such transformation (Figure 5) and the SBI results indicate that it may be necessary to formulate a different set of coefficients for this area. Kauth and Thomas (1976) developed their transformations for cultivated crops and different soil types. A principal component analysis could be used to determine the soil and green vegetation components in South Dakota rangeland. Tucker and Miller (1974) have used regression analysis and ground-based reflectance measurements to extract the soil-based component from the signature of a shortgrass prairie.

Deering et al. (1975) found a significant correlation between a transformed vegetation index (TVI6), based on a ratio of Landsat bands 6 and 5, and rangeland biomass at levels less than 500 kg/ha. The patterns on the 6-5 band ratio index (Figure 6) of Corson County did not appear to be associated with differences in grasshopper density. The

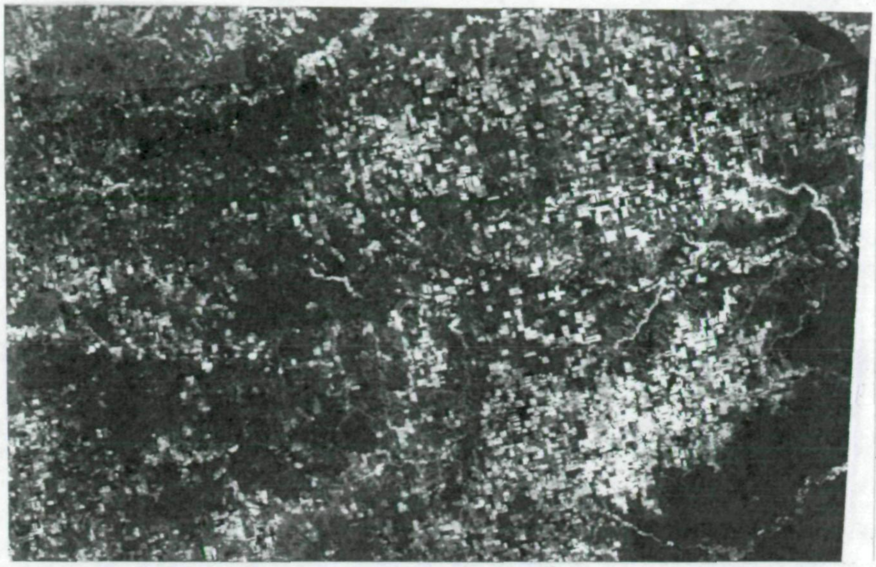

Figure 2. GVI transformation of 9 September 1980 Landsat data for Corson County, South Dakota.

Figure 3. SBI transformation of 9 September 1980 Landsat data for Corson County, South Dakota.

Figure 4. YMI transformation of 9 September 1980 Landsat data for Corson County, South Dakota.

Figure 5. Non-such transformation of 9 September 1980 Landsat data for Corson County, South Dakota.

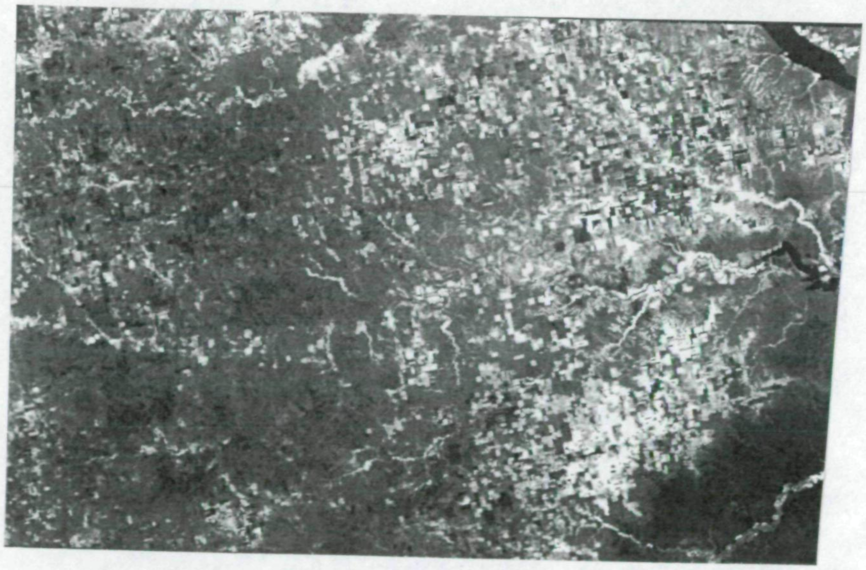

Figure 6. ND 6 index transformation of 9 September 1980 Landsat data for Corson County, South Dakota.

image from this transformation was similar to the GVI image. In both cases, the reflectance differences related to reduced biomass resulting from grasshopper infestations may be too small to be detected within the range of grey tones on an image. A more detailed digital analysis may be necessary.

No patterns associated with grasshopper density were obvious on any of the other band ratio indices tested in this project (Figures 7-11). Investigators have not considered these combinations because the visible bands (4 and 5) and the infrared bands (6 and 7) are generally intercorrelated. There are numerous differences on each of the combinations. Extensive field studies are necessary to determine what these anomalies signify.

Richardson and Wiegand (1977) compared 8 different vegetation index models to field measurements of sorghum fields 6 times during the growing season. The categories correlated to the various Landsat transformations were crop cover, shadow cover, plant height, and Leaf Area Index (LAI). Results showed significant correlation (.01 probability level) of Landsat data with each category except shadow cover. Non-transformed Landsat bands had slightly higher correlation coefficients than any of the transformations; however, several of the transformations did have significant correlation (.01 level) with plant height and LAI. The authors stated that vegetation index models, while having lower correlation coefficients than individual Landsat bands, did have better capability for season-to-season comparisons of vegetation amounts and conditions.

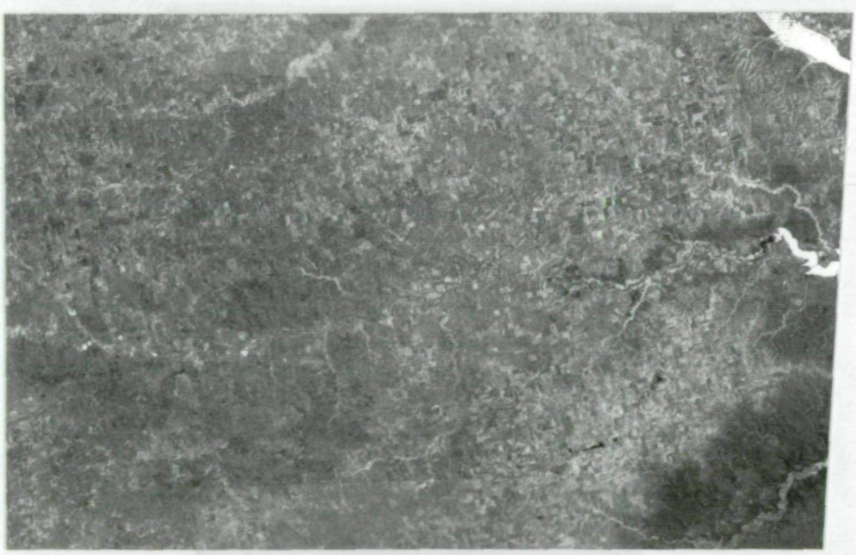

Figure 7. 7-6 bands normalized difference index transformation of 9 September 1980 Landsat data for Corson County, South Dakota.

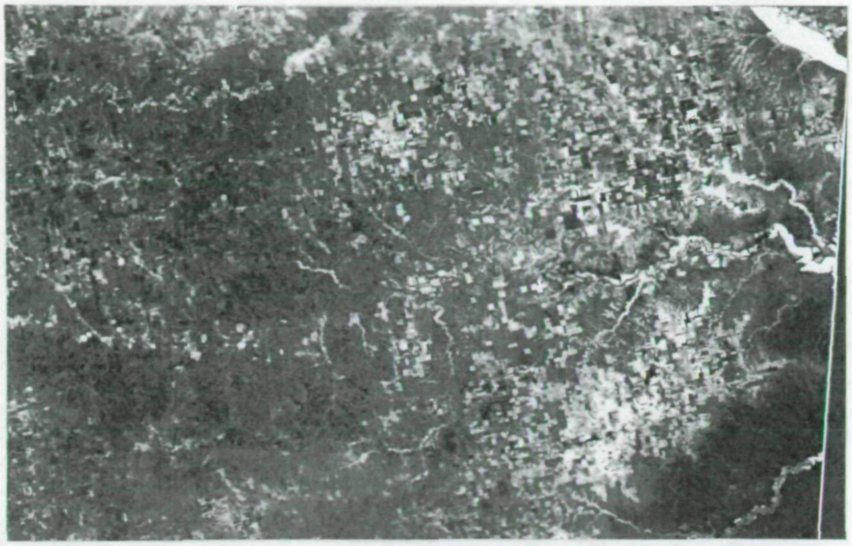

Figure 8. 7-5 band normalized difference index transformation of 9 September 1980 Landsat data for Corson County, South Dakota.

Figure 9. 7-4 band normalized difference index transformation of 9 September 1980 Landsat data for Corson County, South Dakota.

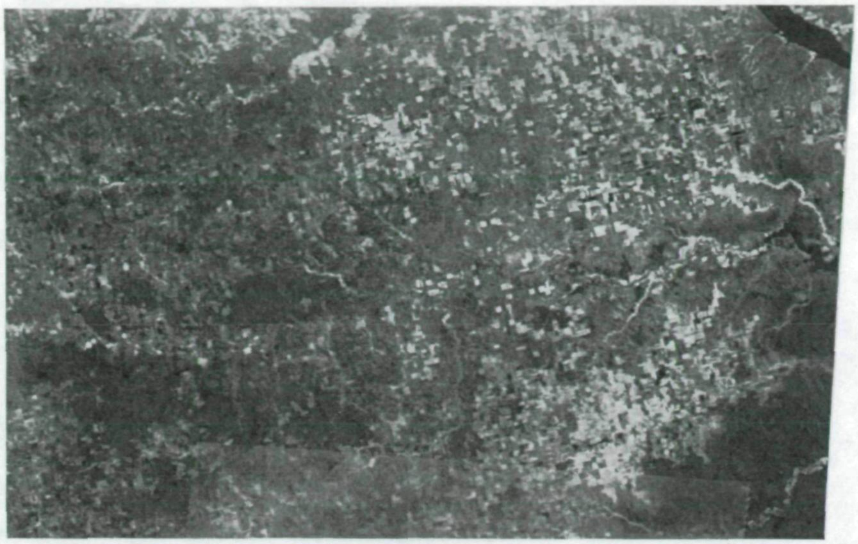

Figure 10. 6-4 band normalized difference index transformation of 9 September 1980 Landsat data for Corson County, South Dakota.

Figure 11. 5-4 band normalized difference index transformation of 9 September 1980 Landsat data for Corson County, South Dakota.

SUMMARY AND CONCLUSION

Subtle tonal differences which may correlate with grasshopper infestations in rangeland were evident on single band MSS imagery. No difference could be visually detected between areas of 3-7 (threatening) and 8 or more (severe) grasshoppers per square yard. Accurate delineations of infested areas could not be made on any date or MSS band on the imagery acquired for this project. No tonal difference relating to grasshopper infestations could be interpreted on the improved resolution RBV imagery acquired for this project.

No patterns associated with reduced biomass resulting from grasshopper infestations could be delineated on any of the vegetative transformations tested in this project. A vegetative component that would correlate with grasshopper density in western rangeland might derivable from a principal component analysis.

If a suitable transformation can be developed it would result in a cost-effective technique for monitoring grasshopper infestations. The technique would be applicable in all western states and would provide data necessary in grasshopper control programs, and would have a sizeable economic impact. The analysis of Landsat data would be used to identify areas of damage and to locate potential sites for large scale spraying programs in the following year.

LITERATURE CITED

Carneggie, D. M. and S. D. De Gloria. 1972. The usefulness of ERTS-1 and supporting aircraft data for monitoring plant development in rangeland environments. pp. 1471-1476 in Proceedings of the 8th International Symposium on Remote Sensing of the Environment, Univ. Michigan, Ann Arbor.

Deering, D. W., J. W. Rouse, R. H. Hass and J. A. Schell. 1975. Measuring "forage production" of grazing units from Landsat MSS data. pp. 1169-1178 in Proceedings of the 10th International Symposium on Remote Sensing of the Environment, ERIM, Ann Arbor, Michigan.

Dougenik, J. A. and D. R. Sheehan. 1977. SYMAP users' reference manual. Laboratory for Computer Graphics and Spatial Analysis, Harvard Univ., Cambridge, Mass., 110 pp.

Harlan, J. C., D. W. Deering, R. H. Haas and W. E. Boyd. 1979. Determination of range biomass using Landsat. pp. 659-673 in Proceedings of the 13th International Symposium on Remote Sensing of the Environment, Univ. Michigan, Ann Arbor.

Hewitt, G. B., W. H. Burleson and J. A. Onsager. 1976. Forage losses caused by the grasshopper *Aulocara* elliotti on shortgrass rangeland. Journal of Range Management 29(5):376-380.

Hielkema, J. U. and J. A. Howard. 1976. Pilot project on the application of remote sensing techniques for improving desert locust survey and control. Food and Agriculture Organization, Rome, Italy. 71 pp.

Kauth, S. J. and G. S. Thomas. 1976. The tasselled cap-agraphic description of the spectral temporal development of agricultural crops as seen by Landsat. Proc. Symp. Machine Proc. of Remote Sensing Data, 4B:41-51, LARS, Purdue Univ., West Lafayette, Ind.

Maxwell, Eugene L. 1976. A remote rangeland analysis system. Journal of Range Manage. 29(1):66-73.

Morton, F. A. 1936. Summary of 1936 grasshopper studies. Bureau of Entomology and Plant Quarantine Laboratory, Bozeman, Mont.

Parker, J. R. 1952. Grasshoppers. pp. 595-605 in Insects: The Yearbook of Agriculture. A. Stefferud ed., U. S. Government Printing Office, Washington, D. C. 780 pp.

Pearson, R. L. and L. D. Miller. 1972. Remote mapping of standing crop biomass for estimation of the productivity of the short grass prairie, Pawnee National Grasslands, Colorado, pp. 1357-1381 in Proceedings of the 8th International Symposium on Remote Sensing of the Environment, Univ. Michigan, Ann Arbor.

Poulton, C. E. 1975. Range resources: inventory, evaluation and monitoring. pp. 1427-1478 in Manual of Remote Sensing Vol. II. R. G. Reeves ed., American Society of Photogrammetry, Falls Church, Virginia.

Richardson, A. J. and C. L. Wiegand. 1977. Distinguishing vegetation from soil background information. Photogram. Eng. and Remote Sensing, Vol. 43(12):1541-1552.

Tucker, C. J. and L. D. Miller. 1974. Extraction of the underlying soil spectra from canopy spectroreflectance measurements of the shortgrass prairie. Proceedings of the 3rd Annual Remote Sensing of Earth Resources, Space Institute, Univ. of Tenn., Tullahoma. (Mimeo)

Tucker, C. J., L. D. Miller and R. L. Pearson. 1975. Short grass prairie spectral measurements. Photogrammetric Eng. and Remote Sensing 41(9):1157-1162.

APPLICATION OF REMOTE SENSING TECHNIQUES FOR DETECTING DUTCH ELM DISEASE IN AN URBAN ENVIRONMENT

By

J. C. Eidenshink

Dutch elm disease is fatal to nearly all elm trees. The disease is transmitted by beetles which survive in the dead or dying trees. Removal of infected trees is the only effective method to contol the disease. Economic loss, including removal of dead trees was $22 million in South Dakota in 1978. The city of Watertown and South Dakota Division of Forestry are cooperating with the Remote Sensing Institute to use remote sensing data for early detection and removal of infected trees before the disease is spread. Color infrared aerial photography and thermal imagery were collected in June and early September, 1980. The June imagery has been interpreted and field checked. Accuracy of the interpretation is most affected by incorrect species identification. September imagery has been interpreted and field checked. Species identification problems were solved but several diseased trees were not identified. It was determined that the use of thermal infrared imagery to detect moisture stress needs further research. Interpretation procedures for aerial photography are recommended.

APPLICATION OF REMOTE SENSING TECHNIQUES FOR DETECTING DUTCH ELM DISEASE IN URBAN ENVIRONMENTS

INTRODUCTION

Dutch elm disease is a disease which is fatal to most elm species, especially the American elm *(Ulmus americana)*. The disease is caused by a fungus *(Cerotocystis ulmi)* which invades and grows in the water conducting vessels of elm. The disease is generally transmitted by the European elm bark bettle *(Scolytus multistriatus)* and the native elm bark bettle *(Hylurgopinus rufipes)*. The beetles overwinter as larvae and adults under the bark of dead or dying elms. In the spring the emerging adult beetles, contaminated with fungus spores, fly to dead or dying trees to reproduce and then on to healthy trees to feed. It is at this point that the infection is spread.

Sanitation by removal and destruction of dead and dying elms is the only way to slow disease spread within an elm population. Prompt identification and destruction can reduce losses to levels where severe economic impact is minimized. The Department of Game, Fish and Parks estimated that 28,000 elms were lost to Dutch elm disease in 1978. The economic loss, including the removal of dead trees, exceeded $22 million.

The severity of the tree loss problem nationwide prompted an investigation to test the feasibility of using aerial color infrared photography for early detection of Dutch elm disease(DED). The investigators determined the disease is easiest to detect and has the highest incidence in early July (French and Meyer, 1977; Waltz, 1969; La Perriere

and Howard, 1971). They also recommended that a survey in late August would be useful for detecting trees infected by second generation adult beetles.

The concensus of the investigators was that aerial photography was a fast, low-cost survey method. Accuracy of detection ranged from 50 to 70 percent. Accuracy was influenced by difficulty in identifying species, discriminating the target disease from other kinds of moisture stress-inducing situations, mapping locations of infected trees and coordinating the photo with the ground situation. It is expected that accuracy can be improved in the proposed project because many of the previous investigations were performed in a natural forest rather than an urban forest. In a normal urban environment it should be easier to identify species because the crown density will be less.

The city of Watertown, South Dakota, with the assistance of the South Dakota Department of Game, Fish and Parks, Division of Forestry, has taken significant preliminary steps to facilitate Dutch elm disease detection. In 1978 the Watertown city forester, with the assistance of the South Dakota Division of Forestry, inventoried the location and species of all trees on public land and street boulevards. The inventory was performed to simplify the annual ground survey which identifies diseased trees on public land.

The main problems presently confronting the city of Watertown are the early identification of diseased elms on private property and the monitoring of elms previously identified as diseased on public property. The process of identifying the diseased trees on private and public land is a conventional ground survey, which is time consuming. The city has

passed an ordinance permitting the city forester to condemn and remove diseased trees on private property at the owner's expense.

The city officials and South Dakota Division of Forestry are hopeful that remote sensing techniques can significantly reduce the amount of time and expense needed to perform the survey of private trees. They are cooperating with the Remote Sensing Institute to develop procedures for an operational program.

The project was originally proposed to begin in 1979. However, weather conditions and equipment malfunctions restricted any data collection until September of 1979. A camera malfunction severely overexposed approximately half of each frame of the film resulting in the film being of minimal use for an operational disease detection program. The project was continued in 1980.

PROCEDURES

On June 23, 1980 a preliminary ground inspection was conducted to obtain ground truth information for a sample area within the city of Watertown. At that time nearly 50 trees were identified as having DED.

On June 28, 1980 1:4,500 scale, 9 x 9 inch color infrared stereo aerial photography of the city was collected. Aerial thermal infrared imagery was also collected over a test site within the city. The imagery was used to delineate trees newly infected with DED during the period from the city-wide survey during the previous fall season throughout the Spring to June 28.

The color infrared photographs were interpreted by two interpreters with only minimal prior experience. The experience of the interpreters was considered to be typical of the experience of a person in a city

forestry position who had some basic training.

The 1:4,500 scale color infrared transparencies were viewed stereoscopically using a 3X enlargement mirror stereoscope. A 6X enlargement was often used in areas where the tree canopy was dense.

Each interpreter used the 50 diseased trees identified in the preliminary ground inspection as a training sample to learn how to interpret trees infected with DED. The first interpreter circled suspected trees. The circles were made on mylar which overlaid the 1:4,500 scale transparencies. After the first interpretation was completed the second interpreter circled any additional infected elm trees missed by the first interpreter.

The two interpreters reviewed the film jointly to discuss any misinterpretations made by either. This process eliminated some misclassifications based generally on species identification.

The major streets were delineated on the mylar overlays to assist the ground crews in locating the suspected trees. Contact prints were made of the transparencies and overlays. The prints were provided to the city of Watertown for verification.

The verification process involved a ground survey of segments of the city. Two areas within the city were ground checked for infected trees. The Watertown City Forester accompanied the ground crew to assist in verification.

On September 2, 1980, 1:4,500 scale 9 x 9 inch color infrared stereo aerial photography of the city was collected, Aerial thermal infrared imagery was again collected over a test site within the city. The photography was used to identify trees infected by DED from late June, 1980 through September 2, 1980.

The photographs were interpreted by an experienced photo interpreter using a mirror stereoscope and 3X-6X enlargement. The photographs were interpretted twice. The first time only trees with a very high probability of having the disease were delineated. The most apprently infected trees were either leafless or had a very obvious pink to grey color in the canopy. Figure 1 depicts a typical tree identified in the first pass. Figure 2 illustrates how a typical tree appears on the imagery.

On the second interpretation, trees with less obvious indicators were delineated. The trees identified generally had very slight tone differences in the canopy. Figure 3 depicts a typical tree identified in the second pass. Figure 4 illustrates how the typical tree appears on the imagery.

The results of the September data interpretation were field verified by a city forester and ground crew during the annual spring DED survey in the second week in June, 1981.

The thermal infrared imagery collected during the fall flight was processed to determine if canopy temperature differences due to the moisture stress symptoms of DED could be detected. Springtime thermal imagery was not analyzed because of high wind conditions at the time of data collection. The wind caused a great deal of canopy motion which camouflaged any temperature differences.

The fall thermal infrared data was collected at 1500 ft. above ground level (AGL) for two temperature ranges: $10^{o}C$-$35^{o}C$ and $8^{o}C$-$30^{o}C$. It was anticipated that the temperature ranges obtained would bracket the apparent temperature of the tree canopy.

Figure 1. American elm which is leafless and dead from DED.

Figure 2. Leafless elm tree as it appears on the imagery.

Figure 3. American elm with wilted leaves - an early sign of DED.

Figure 4. Infected elm tree with leaf wilt as it appears on the imagery.

Black and white imagery were produced from the thermal data. The 10^{o} - $35^{o}C$ apparent temperature range data was utilized. The imagery depicts the total temperature range with 8 equal temperature increments. Table 1 shows the apparent temperature range for each of the 8 levels.

Table 1. Full range apparent temperature levels.

Level	Temperature range (oc)
1	$\leq$ 10.00
2	$\geq$ 10.00 - 14.16
3	$\geq$ 14.16 - 18.33
4	$\geq$ 18.33 - 22.50
5	$\geq$ 22.50 - 26.66
6	$\geq$ 26.66 - 30.83
7	$\geq$ 30.83 - 35.00
8	$\geq$ 35.00

Processing of the thermal data determined that the tree canopy apparent temperature range was 10.00 - $18.33^{o}C$. Several other ground surfaces were also in this apparent temperature range including the lawns. Further processing was done to try and isolate the tree canopy apparent temperatures.

Temperature levels 1 - 3 were expanded into 8 discreet levels in an attempt to isolate the tree canopies. The processing essentially

increased the apparent temperature of the imagery from 4.16°C to 1.388°C. Table 2 shows the temperature range for each of the 8 levels.

Table 2. Apparent temperature range for expanded levels.

Level	Temperature range ($^{\circ}$C)
1	$<$ 10
2	$\geq$ 10 - $<$11.388
3	$\geq$ 11.388 - $<$12.777
4	$\geq$ 12.777 - $<$14.166
5	$\geq$ 14.166 - $<$15.554
6	$\geq$ 15.554 - $<$16.943
7	$\geq$ 16.943 - 18.333
8	$\geq$ 18.333

RESULTS AND DISCUSSION

Approximately 500 trees suspected of having DED were delineated on the interpretation of the June 28, 1980 imagery. Figure 5 is a print of the color infrared imagery with the suspected trees circled. A total of 106 suspected trees were field verified. Sixteen trees not identified during the interpretation were also found during the ground survey and are included in the results. The results are presented in Table 3.

Table 3. Interpretation accuracy of Spring imagery determined by ground verification.

	No.	%
Suspected diseased elms correctly interpreted	50	41
Suspected diseased elms incorrectly interpreted	10	8
Incorrect species interpretation	46	38
Undetected diseased elms	16	13
	122	100

Several Siberian elm were known to be affected by DED. The infected Siberian elm are included in the results. All leafless trees including other species were assumed to be defoliated elm trees. So they are also included in the results.

The accuracy of the interpretation of the Spring data was disappointing, but is similar to other studies (French, 1977). The major problem appears to be specie identification. The resulting error significantly reduces the usefulness of the procedure. The problem is compounded by

Figure 5. Spring color infrared imagery with suspected trees circled.

the fact that some of the elms incorrectly identified as having the disease only appeared so because the canopy of the elm was intermingled with the canopy of another specie. The elm/ash intermingling accounted for the greatest amount of that type of misinterpretation. The color on the imagery of an ash canopy closely resembles that of an elm in the early disease state.

A partial cause of the species misinterpretation was the speed in which the interpretation was made. The interpretation was done as quickly as possible because in an operational program the key factor is removal of diseased trees before the beetles can spread the disease. Fast identification is therefore necessary.

It was anticipated that the amount of overall error and especially the error due to incorrect species identification may be reduced if a careful detailed interpretation was made. Such an interpretation was performed on the fall imagery.

The fall imagery was interpreted by an experienced interpreter. A systematic approach was taken to ensure proper specie identification and disease detection. The first pass interpretation identified 49 suspected trees. Figure 6 is a color infrared print with suspected trees delineated.

The 49 identified trees were an extremely low number in comparison with the Spring results and below what would be expected. This prompted the second interpretation. The second interpretation delineated trees with evidence of minor color variations. The process identified an additional 45 trees for a total of 94.

Figure 6. Fall color infrared imagery with suspected trees circled.

A ground verification of 29 trees showed a significant difference from the Spring data (Table 4).

Table 4. Interpretation accuracy of Fall imagery determined by ground survey.

	No.	%
Suspected Diseased elms correctly interpreted	27	48
Suspected elms incorrectly interpreted	2	4
Incorrect species identification	0	0
Undetected diseased elms	27	48
	56	100

The major improvement of the Fall versus the Spring interpretation is the increase in accuracy due to elimination of species identification error.

The ability to identify which trees are diseased (48%) is misleading however because of the undetected trees. Two factors must be considered in evaluating the 27 undetected trees. First, it is possible the trees became infected after the time of data collection. Secondly, the trees may have been in a very early stage of the disease.

A sample of the unidentified diseased trees were viewed on the imagery to determine if the DED symptoms could be seen after the fact. Fifteen of the twenty-seven trees were viewed. The symptoms of DED could be seen on 5 of 15 trees. No signs whatsoever could be detected in the other 10. It may be concluded that the other 10 trees must have been infected after the time of the fall data collection. If this

conclusion is valid the accuracy is near 60%.

The fact that 49 trees were found in the first interpretation and 45 more in the second interpretation of the fall data indicates that another interpretation may have found some of the trees missed. Perhaps a multiple interpretation in which each successive interpretation would identify trees with a lower probability of having DED. Eventually, an interpreter would develop highly accurate interpretation procedures.

The thermal infrared did not prove to be useful for detection of DED. The primary problem is that the temperature of the lawns was the same as the tree canopy. More research is required to develop a method for determining tree canopy temperatures versus background temperatures and at what time the greatest contrast exists.

SUMMARY AND CONCLUSIONS

The use of low altitude color infrared photography can aid in the identification of elm trees with DED. The accuracy of the photographic interpretation is greatly dependent on the capabilities of the interpreter. An experienced interpreter can accurately identify trees at a level suitable for an operational program.

Thermal infrared data has an application if canopy temperature differences resulting from stress conditions can be detected. However, necessary parameters (time of day, air temperatures, etc.) which would enable detection are not known.

DETERMINATION OF WATER USAGE FROM THE BELLE FOURCHE RIVER

By

J. C. Eidenshink and F. A. Schmer

ABSTRACT

The South Dakota Department of Water and Natural Resources (DWNR) is responsible for allocation and management of water resources for domestic and agricultural use. One area of major concern is the reach of the Belle Fourche River which lies between Keyhole Reservoir in Wyoming and the city of Belle Fourche, South Dakota. This reach of the river is used to transport water from Keyhole Reservoir to the Belle Fourche Reservoir for use by the Belle Fourche Irrigation District. By law, South Dakota has rights to ninety percent of natural flow. It is estimated that over 50% of the water transported to South Dakota is lost before it reaches the Belle Fourche Reservoir. State officials suspect that much of the water is being illegally diverted for irrigation by landowners along the river.

The DWNR requested the Remote Sensing Institute to collect aerial photography to use for identification and documentation of all irrigated land and diversion points along this reach of the river. The irrigated land and diversion points were interpreted from color infrared photography. Color infrared mosaics were produced as base maps of the study area. Irrigated fields acreage and legal descriptions were provided to quantify and document irrigation activity. DWNR will use the data to establish water usage and water rights along the Belle Fourche River study area.

DETERMINATION OF WATER USAGE FROM THE BELLE FOURCHE RIVER

INTRODUCTION

The South Dakota Department of Water and Natural Resources (DWNR), Division of Water Management, Office of Water Rights, is responsible for allocation and management of water resources for domestic and agricultural uses throughout the State. The DWNR coordinates its efforts with local and federal government agencies.

An area of concern for DWNR is the reach of the Belle Fourche River from the city of Belle Fourche in western South Dakota to Keyhole Reservoir in eastern Wyoming. This reach of the river is used to transport water to the Belle Fourche Irrigation District. Water for the Belle Fourche Irrigation District is released from Keyhole Reservoir and stored downriver in the Belle Fourche Reservoir.

The Irrigation District, Bureau of Reclamation and DWNR are very concerned about the diversion of the waters of the Belle Fourche River. Irrigation district officials suspect that unappropriated water is being diverted by irrigators in South Dakota and Wyoming. The diversions are taking place during the times when releases from Keyhole Reservoir are being made to fulfill the District's needs. There is an estimated 50% loss of the water released from Keyhole Reservoir (personal communication). The losses incurred are due to evaporation, percolation into adjacent ground water, diversion for domestic uses and possible illegal diversion for irrigation.

The Irrigation District has the senior appropriative rights to the waters in the Belle Fourche River. The rights have been given to the State of South Dakota by what is known as the Belle Fourche River Compact located in Chapter 46-30 of the South Dakota Compiled laws.

Article V of the compact explains the water rights allocated to each state. As of the date of the compact, the unappropriated waters of the Belle Fourche River are allocated as follows: ninety percent to South Dakota; ten percent to Wyoming with the exception that Wyoming is allowed unrestricted use for domestic and stock use; however, no reservoir for such use shall exceed twenty acre-feet.

The DWNR, Division of Water Management, Office of Water Rights was requested to conduct a survey that would identify what portion of the transportation losses are occurring due to irrigation conducted by existing water rights holders and what portion by irrigators who may be diverting without authorization. The Department of Water and Natural Resources requested the assistance of the Remote Sensing Institute for the acquisition and analysis of aerial photography to provide documentary evidence of pumps, suction lines, canals, and other conveyances for diversion of water along the Belle Fourche River from Keyhole Reservoir to the City of Belle Fourche.

The Department of Water and Natural Resources realizes that research is necessary for determining the best method of accomplishing the tasks described. The Office of Water Rights is cooperating with the Remote Sensing Institute with financial backing and technical support to assist in analyzing aerial imagery that can be utilized to provide the needed documentation.

The results of the project will assist the Water Management Board in evaluating water usage and whether or not this usage is being conducted in an authorized manner. Examination of the records of the State and County will determine the legitimate water right claims. This will lead into the legal settlement of existing water rights to the Belle Fourche River in South Dakota and Wyoming.

STUDY AREA

The study area includes the immediate reach of the Belle Fourche from the Keyhole Reservoir in eastern Wyoming to the City of Belle Fourche in western South Dakota. The river is the primary drainage of the Bear Lodge Mountains, a segment of the Black Hills National Forest. Consequently, the flood plain is often quite narrow and adjacent slopes are often steep and sparsely forested.

PROCEDURES

On July 1, 1980, low altitude 1:61,000 scale stereo color and color infrared aerial photography was collected using the RSI aircraft. The data were collected for the entire study area except for the reach of the river from Keyhole Reservoir downstream 6 miles. Aircraft fuel constraints and unfavorable weather conditions prevented completion. The photography was collected during the period of maximum irrigation water release to ensure the highest probability of irrigation activity.

The aerial photography, in particular the color infrared, was used first to identify irrigated land. Three characteristics were indicative of the irrigated land. First, the area is generally very dry (less than

18 inches of precipitation annually) which causes most vegetation to be under moisture stress by late summer. Consequently, any vegetation reflecting a large amount of infrared light is generally irrigated.

Secondly, much of the irrigation in the study area is flood irrigation. Therefore, most of the field did have easily identifiable berms. Figure 1 illustrates an area of intense flood irrigation. Also note that the presence of berms aided in identifying irrigated fields of recently harvested alfalfa (field A), although recent harvest has significantly reduced the reflected infrared. Field B is an irrigated corn field. The dark portion of the field represents saturated soil due to recent flooding.

The third characteristic which identifies irrigation is field shape. The easiest shape to identify is the circular pattern resulting from center pivot irrigation. Figure 2 illustrates the obvious pattern of a center pivot system in a recently harvested field of alfalfa. Also notice that the darker patterns indicate active sprinkling (see x).

The color infrared photography was utilized to identify the location along the river of the pumps, suction lines, canals and other conveyances used to deliver water to the fields. The possible conveyance sites were determined using several basic principles as indicators of most likely placement of the site. The most basic of the principles is the design of the berm pattern and the fact that the source of water generally will be at the upstream portion of the field.

The 1:61,000 color infrared aerial photography was viewed stereoscopically through a 10x enlarger to pinpoint the precise location of

Figure 1. Area of intense flood irrigation.

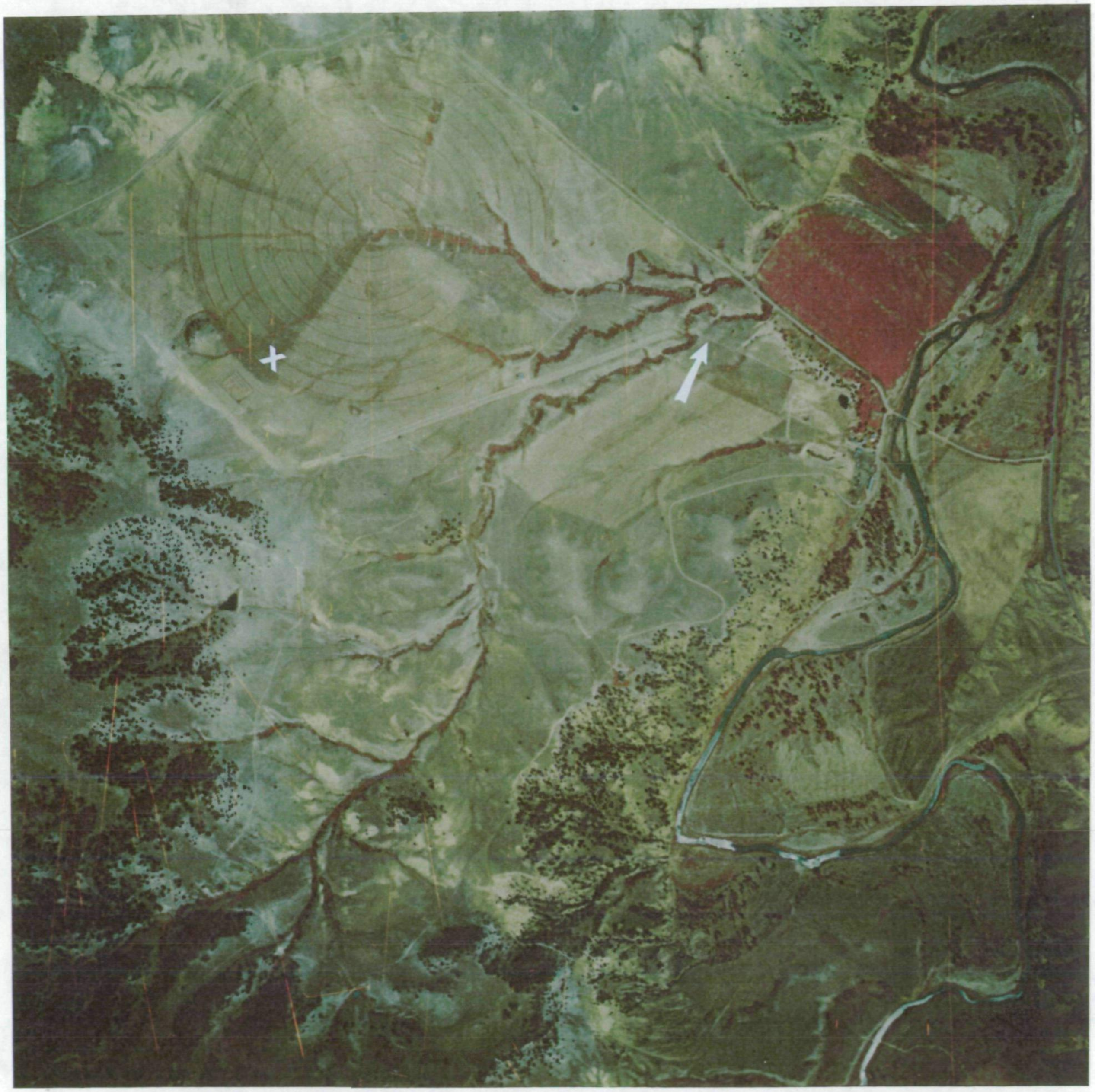

Figure 2. Illustration of the pattern resulting from center pivot irrigation.

the conveyance site. Identification of the specific site was in part due to the disturbance of the natural shoreline which exposed highly reflective sandy soil (Figure 3). Exposure of the soil is due to excavation of the riverbank so that a pump can be placed near enough to the water to pump efficiently. Figures 4 and 5 are typical types of pumps used. Frequently when a pump was removed, the landowner would leave irrigation pipes in place which would help identify the sites (Figure 6 and 7). The existence of the pump itself aided in identifying the site because of the reflectance characteristics of the metal of the pump and aluminum or plastic irrigation pipe.

When pumps were not in place at the time of data collection, as in Figure 3, the sites could be traced by following the ditches used to transport the water (Figure 8) to the point at which the ditches intersected the river.

One other characteristic used to help identify conveyance sites was the evidence of buried pipe. In Figure 2 there is faint evidence of buried pipe deliverying water to the center pivot system (see arrow). The excavation for the pipe has left a scar across the prior homogeneous surface cover resulting in a different spectral reflectance.

The delineation of irrigated land and conveyance sites was plotted on to 1:24,000 USGS orthophotoquads. The orthophotoquads were the only available map source. The base maps were used in the field to complete a field survey of the interpretation. A South Dakota Department of Water and Natural Resources representative accompanied a RSI staff member on the field survey. All identified land and conveyance sites in

Figure 3. Excavation of riverbank to install irrigation pump.

Figure 4. Electric irrigation pump.

Figure 5. PTO driven irrigation pump.

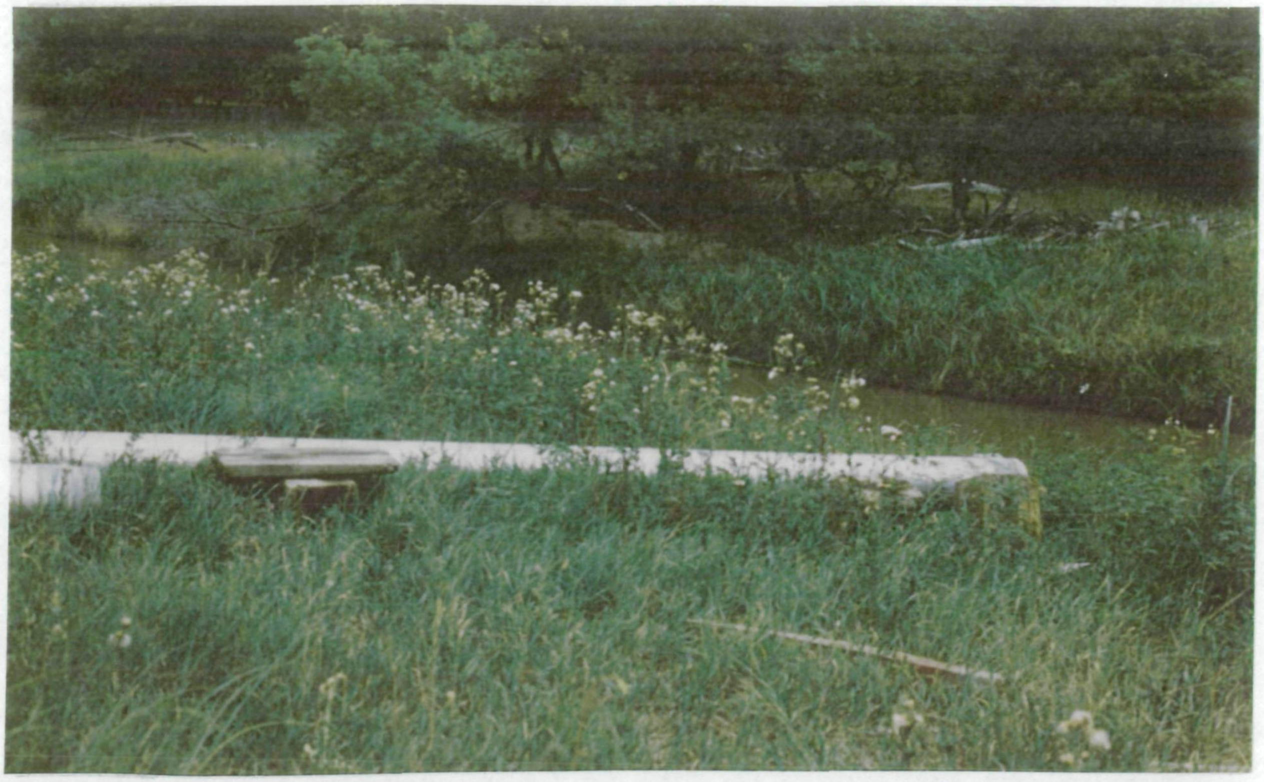

Figure 6. Irrigation pipe left at pump site.

Figure 7. Irrigation pipe left in field.

Figure 8. Irrigation ditch used to transport water for flood irrigation.

the South Dakota portion of the study area were visited and in some cases landowner interviews were conducted. The sites in Wyoming accesible to the public were the only areas visited.

A mosaic utilizing the color infrared photography was produced for use as a new base map of the study area. The mosaic includes all irrigated land adjacent to the river. The mosaic was constructed in eight separate segments because of the length and meandering nature of the river. The scale of the mosaic is approximately 1:16,000 (see Figure 9).

Each individual irrigated land unit was numerically identified on each segment. The numbers were consecutive beginning from the downstream portion near Belle Fourche to the upstream portion near Keyhole Reservoir. The pump sites were also uniquely identified on the mosaic.

The areal extent of each irrigated land unit was measured utilizing an electronic planimeter. A total of 76 individual land units were identified.

The legal description (township, range, section and 1/4 section) was determined for each field. The description was determined by locating each field on a USGS 1:24,000 scale quadrangle. It was also necessary to utilize 1:62,500 scale quadrangles in some areas. In one particular segment the finest resolution map available was a 1:125,000 scale quadrangle.

RESULTS AND DISCUSSION

Field surveys indicated that all irrigated lands were correctly interpreted with the exception of one field of recently harvested alfalfa. Similar results were also achieved in identification of conveyance sites.

Figure 9. Segment of color infrared mosaic with irrigated land units enumerated.

Three 1:16,000 color infrared mosaics were made of the study area. The Department of Water and Natural Resources, the Belle Fourche Irrigation District and the Bureau of Reclamation each received a mosaic. Each also received tabular data of acreage and legal description of each individual irrigated unit (see Appendix A). Each irrigated unit is keyed to a numeric identifier which is present on the mosaic also. This permits easy cross-reference with the mosaic and tabular data.

SUMMARY AND CONCLUSIONS

This projects demonstrates the utility of color infrared photography for identifying irrigated land. The procedures used provided a technically and economically feasible method for evaluating irrigation activity along the Belle Fourche River. The aerial data was especially useful for delineating irrigated land and conveyance sites in this study area because the terrain outside the flood plain is very rugged, the area is quite extensive and access on the ground is very limited. The time needed to interpret and verify the photographs is much less than the amount of time necessary for a detailed ground survey.

The data are being used by the three cooperating agencies to estimate water usage by irrigators adjacent to the river in the study area. Evaluation will be made to determine what portion of South Dakota's water allocation is lost due to riverside irrigation.

The data are also being utilized to determine the legality of each irrigators water rights. The data also provides basic information for establishing future water rights.

APPENDIX A

Legal description and acreage of irrigated land adjacent to the Belle Fourche River.

LEGAL DESCRIPTION AND ACREAGE OF IRRIGATED LAND ADJACENT TO BELLE FOURCHE RIVER FROM BELLE FOURCHE TO NEAR KEYHOLE RESERVOIR

Field No.	Legal Description	Acres
Panel-A 1)	T.9N R.1E. Sec. 31, S.E.¼	93
2)	T.9N R.1E. Sec. 31, S.W.¼	143
3)	T.9N R.1E. Sec. 26, N.W.¼	55
4)	T.9N R.1E. Sec. 23, S.E.¼; Sec. 22 S¼	79
5)	T.9N R.1E. Sec. 22, N.E.¼: S.E.¼	17
6)	T.9N R.1E. Sec. 22, S.E.¼	25
7)	T.9N R.1E. Sec. 22, S.E.¼	15
8)	T.9N R.1E. Sec. 21, S.W.¼	121
9)	T.9N R.1E. Sec. 21, S.E.¼	24
10)	T.9N R.1E. Sec. 21, S.W.¼	24
11)	T.9N R.1E. Sec. 21, S.W.¼; Sec. 20, S.E.¼; Sec. 29, N.E.¼; Sec. 28, N.W.¼	108
12)	T.9N R.1E. Sec. 20, S.E.¼	30
13)	T.9N R.1E. Sec. 20, S.W.¼	133
14)	T.9N R.1E. Sec. 19, S.E.¼	14
15)	T.9N R.1E. Sec. 20, N.W.¼	146
16)	T.9N R.1E. Sec. 20, N.W.¼; Sec. 17, S.W.¼	52
17)	T.9N R.1E. Sec. 18, N.W.¼	85
18)	T.9N R.1E. Sec. 7, S.W.¼; T.55N. R.60W. Sec. 21, N.W.¼	30
Panel-B*19)	T.55N. R.60W. Sec. 17, S.W.¼	180
20)	T.55N. R.60W. Sec. 17, N.W.¼	63
21)	T.55N. R.60W. Sec. 8, S.E.¼	49
22)	T.55N. R.60W. Sec. 7, N.E.¼	47
23)	T.55N. R.60W. Sec. 7, S.W.¼	50
24)	T.55N. R.60W. Sec. 7, S.W.¼	27
25)	T.55N. R.60W. Sec. 7, N.W.¼	25
26)	T.55N. R.60W. Sec. 7, N.W.¼; T.55N. R.61W. Sec. 21, N.E.¼	33

Field No.	Legal Description	Acres
27)	T.55N R.61W. Sec. 12, N.E.¼	71
28)	T.55N R.61W. Sec. 12, N.E.¼	10
29)	T.55N R.61W. Sec. 12, N.E.¼	14
30)	T.55N R.61W. Sec. 1, S.E.¼	26
31)	T.55N R.61W. Sec. 1, S.E.¼	28
32)	T.55N R.61W. Sec. 1, N.W.¼	154
33)	T.55N R.61W. Sec. 1, S.W.¼	81
34)	T.55N R.61W. Sec. 2, N.E.¼	74
35)	T.55N R.61W. Sec. 2, S.W.¼, S.E.¼	106
36)	T.55N R.61W. Sec. 2, S.W.¼	50
37)	T.55N R.61W. Sec. 2, N.W.¼; Sec. 3, N.E.¼	86
38)	T.55N R.61W. Sec. 2, N.W.¼; Sec. 3, N.E.¼	30
39)	T.55N R.61W. Sec. 3, N.E.¼	13
*40)	T.55N R.61W. Sec. 3, N.E.¼	8
*41)	T.55N R.61W. Sec. 3, N.E.¼	32
42)	T.56N R.61W. Sec. 34, N.E.¼	40
*43)	T.56N R.61W. Sec. 34, N.E.¼	18
44)	T.56N R.61W. Sec. 33, S.E.¼	19
45)	T.56N R.61W. Sec. 33, S.E.¼	20
46)	T.56N R.61W. Sec. 29, N.E.¼, S.E.¼, N.W.¼	170
47)	T.56N R.61W. Sec. 29, N.E.¼	30
48)	T.56N R.61W. Sec. 29, N.W.¼	26
49)	T.56N R.61W. Sec. 20, S.W.¼	48
50)	T.56N R.61W. Sec. 20, N.W.¼	71
51)	T.56N R.61W. Sec. 19, N.E.¼	35
52)	T.56N R.61W. Sec. 19, S.E.¼	30
Panel-C 53)	T.56N R.62W. Sec. 13, S.E.¼; Sec. 24, N.E.¼ T.56N R.61W. Sec. 19, N.W.¼	81
54)	T.56N R.62W. Sec. 13, S.E.¼	74
55)	T.57N R.62W. Sec. 26, N.W.¼; S.W.¼	114

Field No.		Legal Description	Acres
Panel-D			
Panel-E	56)	T.56N R.63W. Sec. 29, N.E.¼: S.E.¼	130
Panel-F	57)	T.55N R.64W. Sec. 29, N.E.¼; N.W.¼	55
	58)	T.54N R.64W. Sec. 6, N.W.¼	89
	+59)	T.54N R.64W. Sec. 7, N.W.¼	70
	60)	T.54N R.65W. Sec. 13, N.E.¼, N.W.¼	68
	61)	T.54N R.65W. Sec. 13, N.W.¼	13
	62)	T.54N R.65W. Sec. 12, S.W.¼	113
	63)	T.54N R.65W. Sec. 12, S.W.¼	39
	+64)	T.54N R.65W. Sec. 14, N.E.¼	23
	+65)	T.54N R.65W. Sec. 14, N.E.¼	21
	+66)	T.54N R.65W. Sec. 14, N.E.¼, N.W.¼	104
	+67)	T.54N R.65W. Sec. 14, N.W.¼	103
Panel-G	68)	T.54N R.65W. Sec. 22, N.W.¼	165
	69)	T.54N R.65W. Sec. 28, S.W.¼	71
	69a)	T.54N R.65W. Sec. 29, N.E.¼; Sec. 20, S.E.¼	235
	70)	T.54N R.65W. Sec. 32, N.E.¼, N.W.¼	68
	71)	T.53N R.65W. Sec. 5, S.W.¼; Sec. 8, N.E.¼	233
Panel-H	72)	T.53N R.66W. Sec. 35, S.W.¼	63
	73)	T.52N R.66W. Sec. 2, N.E.¼	92
	74)	T.52N R.66W. Sec. 2, S.W.¼	105
	75)	T.52N R.66W. Sec. 2, S.E.¼	136
	76)	T.52N R.66W. Sec. 1, S.W.¼	63
		TOTAL	5286

RESOURCE MANAGEMENT OF THE LOWER JAMES RIVER WATERSHED

By

J. C. Eidenshink and F. A. Schmer

ABSTRACT

The Lower James Conservancy Sub-District (LJCSD) is primarily responsible for coordinating the management of the lower James River watershed. The complexity of the management problems requires the LJCSD to work closely with several state, local and federal government agencies. The major problems in the immediate reach of the river are stream blockages, streambank erosion and flooding. The LJCSD has requested the assistance of the Remote Sensing Institute in the evaluation and identification of the major and other problems. Low altitude aerial photography was utilized to identify and locate the problem areas. Sandbars, bank erosion, channel obstructions, recreation sites and woodlands were delineated. The location of each delineated area was plotted on 1:24000 scale base maps.

RESOURCE MANAGEMENT OF THE LOWER JAMES RIVER WATERSHED

INTRODUCTION

The Lower James Conservancy Sub-District (LJCSD) is the primary government agency responsible for coordinating the management of the lower James River basin for water development. The Lower James River Conservancy Sub-District encompasses an area in South Dakota, including a 210-mile reach of the river, from the northern Sanborn County line, southward to the confluence of the James and Missouri Rivers near Yankton. The size of the basin is over 2900 square miles.

The size of the area and the complexity of the management problems requires LJCSD to work closely with several local, state and federal governmental agencies and organizations. Those agencies involved include, but are not limited to, the Corps of Engineers; South Dakota Department of Game, Fish and Parks; South Dakota Department of Water and Natural Resource Development; Soil Conservation Service; Lower James Resource Conservation and Development (LJRCD) area; and Third Planning and Development District. A coordinated effort from LJCSD and the numerous other agencies is necessary for good management of the lower James River basin.

The local, state and federal government agencies which have responsibility for water development and management along the reach of the river often deal with several interrelated recurring problems including flooding. As an example, flooding may cause streambank erosion, which in turn will cause uprooted trees to fall into the river channel resulting

in stream blockages that restrict flow and increase the severity of floods.

A major problem in the James River watershed is water quality. Traditional low flows are cited as giving rise to water quality problems (Schmucker, Paul, Nohr and Associates, 1974). The source of water quality problems encompasses the entire watershed of the river. Poor land management, agricultural practices and domestic uses of water will usually result in varying degrees of soil erosion, feedlot runoff and chemical pollution of the river.

The LJCSD in conjunction with the LJRCD area and the Third Planning and Development District requested the Remote Sensing Institute (RSI) to provide assistance and information through the use of remote sensing techniques to aid in the management of the watershed. The objectives of the study were:

(1) Locate and evaluate streambank erosion problems.

(2) Identify existing and potential stream blockages.

(3) Identify woodlands for wildlife habitat and timber industry along the river.

(4) Assist LJCSD and the South Dakota Department of Game, Fish and Parks and other organizations in identifying potential recreation sites along the river.

PROCEDURES

Initially, it was proposed to acquire NASA high altitude aerial photography of the entire watershed. The photography was to be the primary

data source for the study. Unfortunately, timing and weather constraints prohibited data collection.

In response to the nonavailability of NASA imagery, low-altitude 1:61,000-scale stereo color and color infrared aerial photography were collected in July 1980 using the RSI aircraft. The data coverage was of the immediate flood plain of the James River from the northern Sanborn County line to the confluence of the James and Missouri Rivers.

Base maps were produced at a scale of 1:24,000. The base maps were tracings of 1:24,000 USGS 7 1/2 minute quadrangles. The Corps of Engineers' mile numbering system which begins at the mouth of the river and continues upriver was utilized. A two hundred ten mile reach of the river was studied. The 210-mile stretch was divided into 7 sections. The first 4 sections corresponded to the same area studied by Schmucker, Paul, Nohr and Associates in the early 1970's. Some sections are subdivided into subsections called pages.

Woodland, sandbars, bank erosion and snags were interpretted on the color and color infrared photographs. The color infrared imagery was enlarged 3X and viewed stereoscopically to delineate sandbars, snags and bank erosion. Sandbars were very evident on the imagery. Low water levels made even the smallest sandbars visible. In most instances, sandbars were present at the mouths of the tributaries (Figure 1-A).

Streambank erosion problems were identified using two indicators. First, any visible bare soil which usually appeared white was identified as an erosion problem. Secondly, any area with an apparent undercut bank was identified as a problem area. The latter case usually occurred on the outside curve of a meander. These are usually recognized

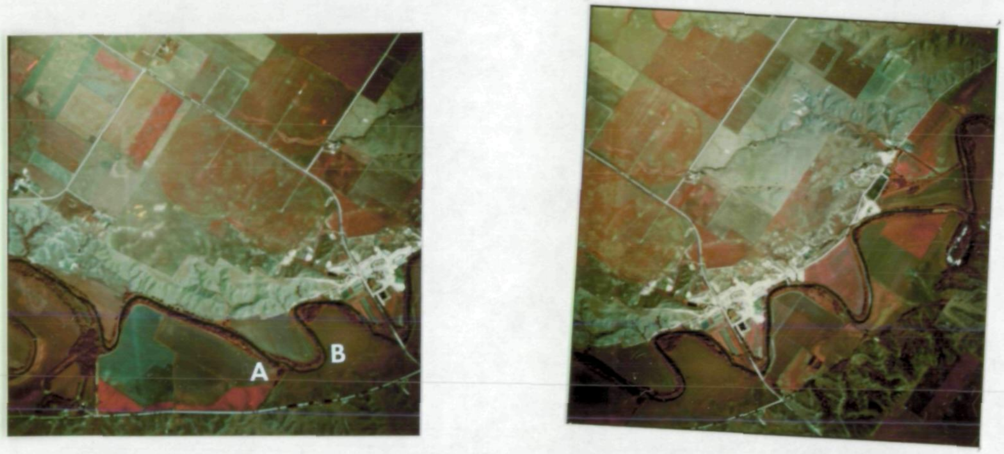

Figure 1. Color infrared stereo pair with evidence of sandbar (A) and bank erosion (B) problems.

stereoscopically because the bank appears vertical. They are also indicated by fallen trees which have been uprooted by the undercutting (Figure 1-B).

Snags were difficult if not impossible to see because of the resolution of the imagery. Along the southern reach of the river there are considerably more trees along the riverbank. Fallen trees were obscured by the existing tree canopy or by shadows. In areas where few trees were present on the riverbank it was possible to partially identify snags in the river channel.

Woodlands are defined as the areas along the riverbank where enough trees exist to be a manageable unit for wildlife habitat or timber. This definition eliminated narrow bands of single trees that are often present. The woodland areas were interpreted from the color photography which was registered to the base maps. The woodland areas were delineated on the base maps. An electronic planimeter was used to calculate the acreage of woodland in the area.

Segments of the channel were studied separately. The interpreter transferred the location of problem areas to the 1:24,000 scale base maps. The base maps were registered to the color photography using a zoom transfer scope. This procedure ensured accurate location of the problem area.

Each problem area was numerically identified. The problem area or obstacle number was part of a table which also included map section and page number, mileage location, type of obstruction, general description and other pertinent information. Sandbars were qualified as either major or minor based on the apparent size. The source of the sandbars, such as bluff erosion or tributary deposits, was also noted.

An attempt was made to evaluate potential recreational sites. Consinderation was given to the river locations where rock dams were present. The dams are approximately 3 feet tall. These small dams serve to maintain a water level upstream which is suitable for recreational purposes.

Information concerning quantitative and qualitative requirements for recreation sites was requested from the South Dakota Department of Game, Fish and Parks. The information was inadequate for evaluation by the investigator. An enlargement print of the Olivet area was produced for assisting in the evaluation.

RESULTS AND DISCUSSION

A total of 569 problem areas were identified along the 210-mile study area. Slightly more than 50% of the problems are related to bank erosion problems. Table 1 includes the pertinent information about each area. Figure 2 is an example of a completed base map.

Table 2 provides a breakdown of the woodland acreage adjacent to the river in each of the counties present in the study area. No specific effort was made to quantify the effects of Dutch Elm disease but it is a significant cause of woodland distribution.

Enlargement prints of a potential recreation site near the town of Olivet have been provided to the LJCSD and the Third Planning and Development District. The photograph will assist in design and development of a proposal for a State recreation site.

The information concerning problem areas, woodland and recreational sites has been provided to the Lower James Conservancy Sub-District and

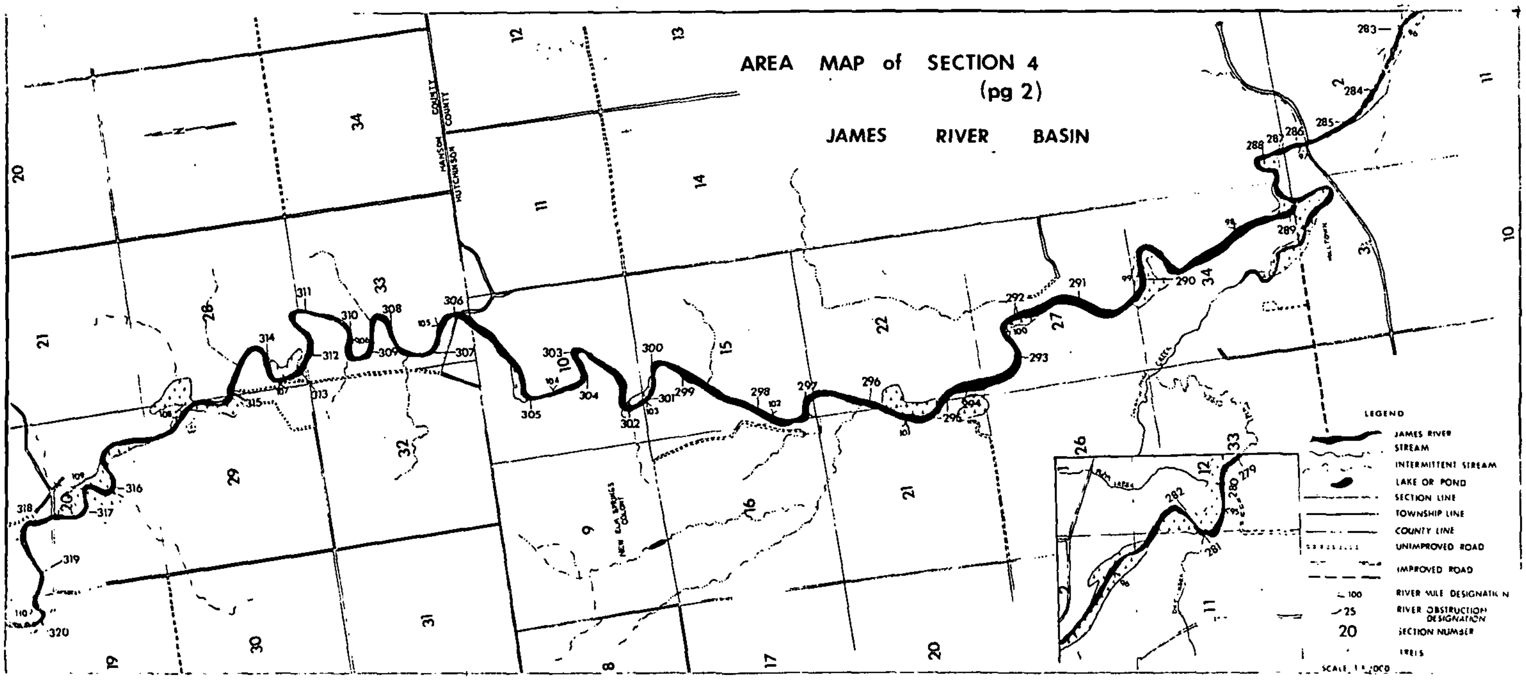

Figure 2. Completed 1:24,000 base map (reduced for publication) with problem sites and woodlands delineated.

Table 1

Obstacle Number	Map Section (Pg.)	River Miles	Type of Obstruction	Description and Estimated Quantity	Notes
1	1-1	6	sand bar	minor blockage	
2	1-1	6.9	erosion	bank undercut	
3	1-1	7.2	trash on bank		
4	1-1	7.9	sand bar	minor-barely emergent	
5	1-1	8.2	erosion	exposed soil	
6	1-1	8.4	erosion	bank undercut	trees on bank
7	1-1	9.1	erosion	sand bar	bank undercut
8	1-1	9.2	sand bar	minor blockage	mouth of stream
9	1-2	9.8	erosion	band undercut	sparse trees
10	1-2	10.4	erosion	bank undercut	trees on bank
11	1-2	10.6	sand bar	major blockage	erosion from bluffs
12	1-2	10.8	sand bar	several minor blockages	
13	1-2	11.2	erosion	exposed soil	
14	1-2	11.4	sand bar	minor-barely emergent	
15	1-2	12.1	erosion	bank undercut	trees on bank
16	1-2	12.5	erosion	bank undercut	bank collapsed livestock watering
17	1-2	13.0	sand bar	major blockages	slightly down river from mouth of stream
18	1-2	13.2	erosion	bank undercut	trees on bank
19	1-2	13.4	erosion	bank undercut	trees on bank
20	1-2	13.8	erosion	bank undercut	trees on bank
21	1-2	14.0	sand bar	major blockage	at mouth of stream
22	1-2	14.5	erosion	bank undercut	trees on bank
23	1-2	14.8	erosion	bank undercut	trees on bank
24	1-2	15.2	sand bar	major blockage	near mouth of stream
25	1-2	15.6	sand bar	minor blockage	near mouth of stream
26	1-2	16.5	sand bar	major blockage	mouth of stream livestock watering
27	1-2	16.9	sand bar	minor blockage	
28	1-2	17.2	erosion	bank undercut	collapsed
29	1-2	17.5	sand bar	major blockage	large size
30	1-2	17.9	sand bar	major blockage	mouth of stream
31	1-2	18.2	sand bar	minor blockage	
32	1-2	18.3	erosion	bank undercut	trees on bank
33	1-2	18.4	erosion	bank undercut	
34	1-2	18.6	sand bar	major blockage	mouth of stream
35	1-2	19.2	erosion	bank undercut	
36	1-2	20.0	erosion	bank undercut	trees on bank
37	1-2	20.4	sand bar	minor blockage	mouth of stream
38	1-2	20.5	erosion	bank undercut	
39	1-2	20.8	erosion	bank undercut	no trees
40	1-2	21.3	erosion	bank undercut	trees on bank
41	1-2	21.4	sand bar	minor blockage	mouth of stream

Table 1 (Continued)

Obstacle Number	Map Section (Pg.)	River Miles	Type of Obstruction	Description and Estimated Quantity	Notes
42	1-2	22.4	rock dam	land owner forge	feedlot runoff possible
43	1-2	22.7	erosion	bank undercut	
44	1-2	23.1	sand bar	major blockage	
45	1-2	23.2	erosion	bank undercut	minor
46	1-2	23.6	sand bar	major blockage	mouth of stream
47	1-2	23.8	sand bar	minor blockage	mouth of stream
48	1-2	24.1	erosion	bank undercut	
49	1-2	24.2	sand bar	minor blockages	3 of them
50	1-2	24.8	erosion	bank undercut	no trees, before bridge broad area
51	1-2	25.1	erosion	bank slope exposed	bare soil/no veg.
52	1-2	25.2	erosion	bank undercut	
53	1-2	25.3	sand bar	deposits from bluff	small
54	1-2	25.4	sand bar	deposits from bluff	small
55	1-2	25.5	sand bar	deposits from bluff	very small
56	2-1	25.9	erosion	bare soil	
57	2-1	26.3	sand bar	major	
58	2-1	26.6	erosion	slope steep	probable drainage from farm
59	2-1	26.8	erosion	bank undercut	
60	2-1	26.9	sand bar	major	
61	2-1	27.2	erosion	bank undercut	bare bank
62	2-1	27.5	erosion	bank undercut	
63	2-1	27.6	sand bar	major	
64	2-1	28	sand bar	major	
65	2-1	28.1	erosion	bank undercut	
66	2-1	28.5	sand bar	minor	
67	2-1	28.8	sand bar	major	at mouth of stream
68	2-1	29.1	erosion	bare soil	
69	2-1	29.4	sand bar	minor	at mouth of stream
70	2-1	29.7	erosion	bank undercut	
71	2-1	29.8	sand bar	major	
72	2-1	30	sand bar	major	
73	2-1	30.1	sand bar	minor	
74	2-1	30.2	erosion	bank undercut	
75	2-1	30.5	erosion	bank undercut	
76	2-1	30.7	erosion	bank undercut	
77	2-1	31	erosion	bank undercut	
78	2-1	31.3	erosion	bank undercut	
79	2-1	31.5	erosion	bare soil	
80	2-1	31.6	erosion	bank undercut	
81	2-1	32	erosion	bank undercut	
82	2-1	32.4	erosion	bare soil	

Table 1 (Continued)

Obstacle Number	Map Section (Pg.)	River Miles	Type of Obstruction	Description and Estimated Quantity	Notes
83	2-1	32.6	erosion	bank undercut	
84	2-1	33.5	erosion	bank undercut	
85	2-1	33.6	erosion	bare soil	
86	2-1	34.3	sand bar	minor	at mouth of stream
87	2-1	34.5	erosion	bank undercut	some trees
88	2-1	34.6	sand bar	major	
89	2-1	35.1	sand bar	minor	
90	2-1	35.2	sand bar	minor	
91	2-1	35.6	erosion	bank undercut	
92	2-1	36	sand bar	minor	
93	2-1	36.5	erosion	bank undercut	
94	2-1	36.7	sand bar	major	
95	2-1	37.1	sand bar	minor	
96	2-1	37.2	erosion	bank undercut	
97	2-1	37.5	erosion	bank undercut	
98	2-1	37.7	sand bar	minor	
99	2-1	39	erosion	bank undercut	
100	2-1	39.2	sand bar	minor	
101	2-1	39.3	sand bar	major	
102	2-1	39.7	sand bar	minor	mouth of stream
103	2-1	40.3	sand bar	major	
104	2-1	41	erosion	bank undercut	
105	2-1	41.1	erosion	bare soil	
106	2-1	41.3	sand bar	two minor	
107	2-1	41.8	erosion	bank undercut	
108	2-1	42.6	erosion	bank undercut	
109	2-1	42.6	sand bar	major	
110	2-1	42.7	erosion	bank undercut	trees in river
111	2-1	43.3	sand bar	minor	mouth of stream
112	2-1	43.4	erosion	bank undercut	trees on bank
113	2-1	43.5	erosion	bank undercut	trees on bank
114	2-1	43.8	sand bar	major - bank under-	trees
115	2-1	44.1	sand bar	major /cut	mouth of stream
116	2-1	44.2	erosion	bank undercut	trees on bank
117	2-1	44.3	erosion	bank undercut	trees on bank
118	2-1	4.55	erosion	bank undercut	
119	2-1	45.8	erosion	bank undercut	
120	2-1	46.0	sand bar	minor	mouth of stream
121	2-1	46.2	erosion	bank undercut	trees on bank
122	2-1	46.3	sand bar	major	
123	2-1	46.4	sand bar	minor	
124	2-1	46.5	erosion	bank undercut	trees on bank
125	2-1	46.8	sand bar	major	
126	2-2	47.1	erosion	bank undercut	trees on bank
127	2-2	47.2	sand bar	major	mouth of stream

Table 1 (Continued)

Obstacle Number	Map Section (Pg.)	River Miles	Type of Obstruction	Description and Estimated Quantity	Notes
128	2-2	47.7	feedlot	draining into river	
129	2-2	47.8	erosion	bank undercut	
130	2-2	48.5	sand bar	minor	near bridge
131	2-2	48.9	erosion	bank undercut	bare bank
132	2-2	49.1	sand bar	major	mouth of stream
133	2-2	49.9	sand bar	minor	mouth of stream
134	2-2	50.1	erosion	bank undercut	bare bank
135	2-2	50.2	sand bar	major	
136	2-2	50.5	erosion	bank undercut	trees on bank
137	2-2	50.9	erosion	bank undercut	trees on bank
138	2-2	51	sand bar	ajor	mouth of stream
139	2-2	51.3	erosion	bank undercut	bare bank
140	2-2	51.5	erosion	bank undercut	trees on bank
141	2-2	51.6	erosion	bank undercut	trees on bank
142	2-2	51.7	sand bar	major	mouth of stream
143	2-2	52.2	erosion	bank undercut	few trees on bank
144	2-2	52.8	sand bar	minor	mouth of stream
145	2-2	53	erosion	bank undercut	exposed soil
146	2-2	53.4	erosion	bank undercut	trees on bank
147	2-2	53.8	sand bar	minor	mouth of stream
148	2-2	54.1	sand bar	major	mouth of stream
149	2-2	54.2	rock dam		near water
150	2-2	54.6	erosion	bank undercut	treatment pond
151	2-2	55.4	erosion	bank undercut	very little veg.
152	2-2	56.2	erosio	bank undercut	bare soil
153	2-2	56.4	erosion	bank undercut	bare soil
154	2-2	56.9	erosion	bank undercut	few trees
155	2-2	57.2	erosion	bank undercut	no trees
156	2-2	57.5	erosion	bank undercut	few trees
157	2-2	58.2	erosion	bank undercut	bare soil
158	2-2	58.4	erosion	bank undercut	few trees
159	2-2	58.7	erosion	bank undercut	few trees
160	2-2	59.4	erosion	bank undercut	no trees
161	2-2	59.8	erosion	bank undercut	few trees - snags
162	2-2	60.2	erosion	bank undercut	trees on bank snags
163	2-2	60.5	erosion.	bank undercut	few trees - snags
164	2-2	60.6	erosion	minor	mouth of stream
165	2-2	61.0	erosion	bank undercut	no veg. - snags
166	2-2	61.3	erosion	bank undercut	few trees - snags
167	2-2	61.4	erosion	bank undercut	snags
168	2-2	61.6	erosion	bank undercut	no veg. - snags
169	2-2	61.9	erosion	bank undercut	no vegetation
170	2-2	62.0	erosion	bank undercut	bank collapsed
171	2-2	62.1	sand bar	minor	

Table 1 (Continued)

Obstacle Number	Map Section (Pg.)	River Miles	Type of Obstruction	Description and Estimated Quantity	Notes
172	2-2	62.3	erosion	bank undercut	
173	2-2	62.5	sand bar	minor	
174	2-2	62.5	erosion	bank collapsed	
175	2-2	62.7	erosion	bank collapsed	
176	2-2	62.8	sand bar		shallow area center of stream
177	2-2	63.1	erosion	bank collapsed	
178	2-2	63.3	erosion	bank undercut	snags
179	2-2	63.6	rock dam	major blockage	
180	3	64.4	erosion	bank undercut	steep, barren
181	3	64.5	erosion	bank undercut	snags
182	3	64.6	erosion	bank undercut	snags
183	3	65.1	erosion	bank undercut	snags
184	3	65.5	erosion	bank undercut	large area
185	3	65.8	erosion	bare soil	
186	3	66	erosion	bank undercut	snags
187	3	66.1	erosion	bank collapsed	
188	3	67	erosion		
189	3	67.2	snags	numerous	dead trees
190	3	67.9	erosion	slope barren	no vegetation
191	3	68	erosion	bank undercut	
192	3	68.5	erosion	exposed soil	
193	3	68.7	erosion	bank undercut	snags
194	3	68.9	erosion	bank undercut	snags
195	3	69.1	erosion	bank undercut	snags
196	3	69.5	sand bar	minor	
197	3	69.6	erosion	bank undercut	snags
198	3	69.7	erosion	bank undercut	snags
199	3	69.8	erosion	bank undercut	trees on bank
200	3	70.1	erosion	bank undercut	trees on bank
201	3	70.6	erosion	bank undercut	snags
202	3	71.2	erosion	bank undercut	
203	3	71.4	sand bar	major	at mouth of stream
204	3	71.5	erosion	bank undercut	snags
205	3	72.1	erosion	bank undercut	snags
206	3	72.2	sand bar	major	
207	3	72.4	erosion	bank undercut	snags, trees
208	3	72.5	erosion	bare soil	
209	3	72.5	sand bar	minor	
210	3	72.6	sand bar	major	
211	3	72.6	sand bar	major	
212	3	73.1	erosion	bank undercut	snags
213	3	73.2	sand bar	minor	

Table 1 (Continued)

Obstacle Number	Map Section (Pg.)	River Miles	Type of Obstruction	Description and Estimated Quantity	Notes
214	3	73.3	sand bar	major	at mouth of stream
215	3	73.4	erosion	bare soil	
216	3	73.5	sand bar	minor	at mouth of stream
217	3	74	erosion	bare soil	
218	3	74.4	erosion	exposed bank	
219	3	74.45	sand bar	minor	
220	3	74.5	erosion	bank undercut	
221	3	74.7	erosion	bank undercut	
222	3	74.75	sand bar	major	
223	3	74.8	erosion	bank undercut	snags
224	3	74.9	erosion	bank undercut	
225	3	75.1	snag		
226	3	75.2	snag		
227	3	75.3	sand bar	major	at mouth of stream
228	3	75.4	sand bars	series of 3 major	
229	3	75.5	erosion	banks collapsed	
230	3	75.6	sand bars	series of minor	shallow
231	3	75.8	erosion	both sides	
232	3	75.9	sand bar		
233	3	75.95	snags		
234	3	76	erosion	banks collapsed	
235	3	76.1	sand bars	major series	
236	3	76.5	sand bars		
237	3	76.6	erosion		
238	3	76.8	sand bar		
239	3	76.95	rock dam		
240	3	79.4	erosion	collapsed bank	mouth of stream
241	3	79.5	erosion	bank undercut	
242	3	79.9	erosion		
243	3	80.1	erosion	larger area	vacant of veg.
244	3	81.1	erosion	on bank	
245	3	81.6	erosion	bank undercut	
246	3	81.9	erosion	banks undercut	snag
247	3	82.4	sand bar	minor	
248	3	82.5	erosion	bank undercut	
249	3	82.9	erosion	bank undercut	trees on bank
250	3	83	erosion	exposed soil	
251	4-1	83.7	erosion	bank undercut	
252	4-1	83.8	erosion	bank undercut	snags
253	4-1	84	erosion	bank undercut	
254	4-1	84.1	erosion	bank undercut	snags
255	4-1	84.5	erosion	bank undercut	snags, bare bank

Table 1 (Continued)

Obstacle Number	Map Section (Pg.)	River Miles	Type of Obstruction	Description and Estimated Quantity	Notes
256	4-1	84.9	erosion	vacant of veg.	bare banks
257	4-1	85.8	erosion	bank undercut	
258	4-1	86	sand bar	minor	
259	4-1	86.2	erosion	bank undercut	
260	4-1	86.5	sand bar	minor	
261	4-1	87.4	sand bar		
262	4-1	88	erosion	bank undercut	exposed banks
263	4-1	88.4	erosion	bank undercut	
264	4-1	88.9	erosion	collapsed banks	
265	4-1	89.2	erosion	bank undercut	
266	4-1	89.4	sand bar	minor	
267	4-1	89.9	erosion	bank undercut	snags
268	4-1	90	sand bar	major	
269	4-1	90.1	sand bar	minor	
270	4-1	90.3	erosion	bank undercut	no vegetation
271	4-1	90.5	sand bar	minor	
272	4-1	91.1	sand bar	major	mouth of stream
273	4-1	91.3	erosion	bank undercut	no veg. on banks
274	4-1	91.5	erosion	bank undercut	
275	4-1	92.5	erosion	bank undercut	
276	4-1	92.6	sand bar	major	
277	4-1	93	erosion	bank undercut	trees on bank
278	4-1	93.5	sand bar	series of minor	
279	4-1	94.3	erosion	bank undercut	bare banks
280	4-1	94.5	erosion	banks vacant of veg.	
281	4-1	95.1	sand bar	major	
282	4-1	95.2	erosion	bank undercut	
283	4-2	96	sand bar	minor	
284	4-2	96.5	erosion	bank undercut	
285	4-2	96.6	erosion	bank undercut	
286	4-2	97	erosion	bank undercut	
287	4-2	97	erosion	bank undercut	
288	4-2	97.3	erosion	exposed soil	
289	4-2	97.8	erosion	bank undercut	
290	4-2	99	erosion	bank undercut	
291	4-2	99.5	erosion	bank undercut	exposed soil
292	4-2	100	erosion	bank undercut	
293	4-2	100.2	sand bar	minor	
294	4-2	100.6	erosion	bank undercut	
295	4-2	100.7	erosion	bank undercut	
296	4-2	101.4	sand bar	major	
297	4-2	101.7	erosion	bank undercut	
298	4-2	102.1	sand bar	major	
299	4-2	102.8	sand bar	major	at mouth of stream

Table 1 (Continued)

Obstacle Number	Map Section (Pg.)	River Miles	Type of Obstruction	Description and Estimated Quantity	Notes
300	4-2	102.8	erosion	bank undercut	
301	4-2	103	erosion	bank undercut	
302	4-2	103.1	erosion	bank undercut	
303	4-2	103.7	sand bar	minor	barren banks
304	4-2	103.8	sand bar	minor	
305	4-2	104.1	erosion	bank undercut	
306	4-2	104.9	rock dam		
307	4-2	105.1	erosion	exposed soil	
308	4-2	105.5	erosion	both sides of river	barren banks
309	4-2	105.8	erosion		barren banks
310	4-2	106.1	erosion	bank undercut	
311	4-2	106.5	erosion	bank undercut	
312	4-2	106.7	erosion	bank undercut	
313	4-2	106.8	erosion	exposed banks	
314	4-2	107.1	erosion	bank undercut	trees on banks
315	4-2	107.5	sand bar	minor	
316	4-2	108.8	erosion	bank undercut	
317	4-2	109.1	erosion	bank undercut	
318	5-1	109.4	erosion	bank undercut	
319	5-1	109.8	erosion	bank undercut	
320	5-1	110.1	erosion	bank undercut	
321	5-1	110.4	erosion	bank undercut	
322	5-1	111.1	erosion	exposed soil	
323	5-1	111.3	erosion	bank undercut	
324	5-1	111.8	erosion	bank undercut	
325	5-1	112.3	erosion	bare banks, undercut	
326	5-1	113.5	erosion	bank undercut	
327	5-1	114.2	sand bar	minor	
328	5-1	114.8	erosion	bank undercut	
329	5-1	115	erosion	bank undercut	
330	5-1	115.8	sand bar	major	
331	5-1	116.3	erosion	bank undercut	
332	5-1	116.4	sand bar	major	
333	5-1	116.8	sand bar	major	at mouth of stream
334	5-1	117	erosion	bank undercut	
335	5-1	117.1	erosion	bank undercut	
336	5-1	117.4	erosion	bank undercut	
337	5-1	118.2	sand bar	minor	bare banks
338	5-1	118.3	sand bar	minor	
339	5-1	118.8	erosion	bank undercut	
340	5-1	119.1	dam		
341	5-1	120.1	erosion	soil exposed	
342	5-1	120.5	erosion	bare banks	
343	5-1	121.2	erosion	bare banks	

Table 1 (Continued)

Obstacle Number	Map Section (Pg.)	River Miles	Type of Obstruction	Description and Estimated Quantity	Notes
344	5-1	121.5	erosion	bank undercut	bare banks
345	5-1	122.1	erosion	bank undercut	
346	5-1	123	erosion	bank undercut	
347	5-1	123.9	erosion	exposed banks	
348	5-1	125	erosion	bank undercut	trees on banks
349	5-1	126	sand bar	minor	
350	5-1	126.1	erosion	bank undercut	
351	5-1	127.1	erosion	bank undercut	
352	5-1	127.9	erosion	bank undercut	
353	5-1	128.5	erosion	bank undercut	
354	5-1	129.8	erosion	bank undercut	
355	5-2	130.8	erosion	bank undercut	
356	5-2	131.5	erosion	bank undercut	
357	5-2	132	erosion	bank undercut	
358	5-2	132.2	erosion	bank undercut	
359	5-2	133.1	erosion	bank undercut	
360	5-2	133.8	erosion	bank undercut	trees on bank
361	5-2	134.1	erosion	bank undercut	
362	5-2	135.1	erosion	exposed soil	
363	5-2	135.8	erosion	bank undercut	trees and snags
364	5-2	136	sand bar	minor	
365	5-2	136.5	erosion	bank undercut	trees on banks
366	5-2	137	erosion	bank undercut	trees on banks
367	5-2	137.3	erosion	bank undercut	
368	5-2	137.6	erosion	snags	
369	5-2	137.8	erosion	bank undercut	
370	5-2	138.2	erosion	bank undercut	trees and snags
371	5-2	138.6	erosion	bank undercut	
372	5-2	138.8	erosion	exposed soil on banks	
373	5-2	139.1	erosion	bank undercut	trees and snags
374	5-2	139.2	erosion		
375	5-2	139.9	sand bar	major	at mouth of stream
376	5-2	140.1	sand bar	minor	
377	5-2	140.2	sand bar	major	
378	5-2	140.5	erosion	bank undercut	
379	5-2	140.9	erosion	bank undercut	
380	5-2	142	erosion	bank undercut	snags
381	5-2	142.5	erosion	bank undercut	trees on banks
382	5-2	142.8	erosion	bank undercut	
383	5-2	142.9	erosion	exposed soil	
384	5-2	143.1	erosion	bank undercut	
385	5-2	143.8	erosion	bank undercut	snags
386	5-2	144.1	dam		
387	5-2	144.2	erosion	banks collapsed	
388	5-2	144.3	erosion	bank undercut	

Table 1 (Continued)

Obstacle Number	Map Section (Pg.)	River Miles	Type of Obstruction	Description and Estimated Quantity	Notes
389	5-2	144.7	erosion	bank undercut	
390	5-2	145.2	erosion	bank undercut	snags
391	5-2	145.5	erosion	bank undercut	
392	5-2	145.8	erosion	snags	
393	5-2	146.1	erosion	bank undercut	
394	5-2	147.2	erosion	bank undercut	
395	6-1	148.6	erosion	exposed soil	
396	6-1	148.9	erosion	bank undercut	
397	6-1	149.1	erosion	bank collapsed	
398	6-1	149.4	erosion	bank undercut	
399	6-1	150	erosion	bank undercut	
400	6-1	150.2	erosion	bank undercut	
401	6-1	150.3	erosion	bank undercut	
402	6-1	151.1	erosion	exposed soil	
403	6-1	151.4	erosion	bank undercut	
404	6-1	152.5	erosion	exposed soil	
405	6-1	152.7	erosion	bank undercut	
406	6-1	153.2	sand bar	minor	
407	6-1	153.2	bridge or dam		
408	6-1	153.6	erosion	bank undercut	
409	6-1	153.8	erosion	exposed soil	
410	6-1	153.9	erosion	bank undercut	
411	6-1	154.6	erosion	exposed soil	
412	6-1	154.8	erosion	bank undercut	
413	6-1	155.6	erosion	bank undercut	
414	6-1	155.9	erosion	exposed soil on banks	
415	6-1	156	erosion	bank undercut	
416	6-1	156.3	sand bar	minor	
417	6-1	156.4	erosion	bank undercut	
418	6-1	156.8	erosion	bank undercut	
419	6-1	157.5	erosion	bank undercut	
420	6-1	158	erosion	bank undercut	
421	6-1	158.5	erosion	bank undercut	
422	6-1	158.9	erosion	bank undercut	
423	6-1	159.2	erosion	bank undercut	
424	6-1	159.9	sand bar	major	
425	6-1	160.5	erosion	bank undercut	
426	6-1	160.6	erosion	bank undercut	
427	6-1	161.5	erosion	bank undercut	
428	6-1	161.9	erosion	bank undercut	
429	6-1	162.5	erosion	bank undercut	
430	6-1	163	erosion	bank undercut	
431	6-1	163.5	sand bar	minor	
432	6-1	163.6	erosion	exposed soil	

Table 1 (Continued)

Obstacle Number	Map Section (Pg.)	River Miles	Type of Obstruction	Description and Estimated Quantity	Notes
433	6-1	163.9	erosion	bank undercut	
434	6-1	164.1	erosion	exposed soil	
435	6-1	164.4	erosion	bank undercut	
436	6-1	164.8	erosion	bank undercut	
437	6-1	165.4	erosion	bank undercut	
438	6-2	165.9	erosion	banks collapsed	
439	6-2	166.9	erosion	bank undercut	
440	6-2	168	sand bar	minor	
441	6-2	168.4	erosion	exposed banks	
442	6-2	168.6	sand bar	major	
443	6-2	168.9	erosion	bank undercut	
444	6-2	169	sand bar	minor	
445	6-2	169.2	sand bar	minor	
446	6-2	169.5	erosion	bank undercut	
447	6-2	169.8	erosion	banks collapsed	
448	6-2	170.1	sand bar	minor	
449	6-2	170.4	erosion	bank undercut	
450	6-2	170.8	sand bars	minor	
451	6-2	171.1	erosion	bank undercut	
452	6-2	171.4	erosion	banks collapsed	
453	6-2	171.5	sand bars	series of major	
454	6-2	171.8	sand bar	minor	
455	6-2	172.1	erosion	exposed soil	
456	6-2	172.4	erosion	banks undercut	
457	6-2	172.6	sand bar	major	
458	6-2	172.7	sand bar	minor	
459	6-2	173.1	erosion	bank undercut	
460	6-2	173.4	erosion	bank undercut	
461	6-2	173.8	sand bar	minor	
462	6-2	174.2	sand bar	minor	
463	6-2	174.4	sand bar	major	
464	6-2	174.8	sand bar	minor	
465	6-2	174.85	dam		
466	6-2	175	erosion	bank undercut	
467	6-2	175.5	erosion	bank undercut	
468	6-2	176	sand bar	minor	
469	6-2	177	erosion	bank undercut	
470	6-2	177.3	sand bar	minor	
471	6-2	177.5	sand bar	minor	
472	6-2	177.7	sand bar	major	
473	6-2	178	sand bar	major	
474	6-2	178.2	sand bar	major	
475	6-2	178.8	erosion	bank undercut	
476	6-2	179.1	erosion	bank undercut	

Table 1 (Continued)

Obstacle Number	Map Section (Pg.)	River Miles	Type of Obstruction	Description and Estimated Quantity	Notes
477	7-1	180	erosion	bank undercut	
478	7-1	182.2	erosion	bank undercut	
479	7-1	182.4	sand bars	series of minor	
480	7-1	183.1	erosion	bank undercut	
481	7-1	183.8	sand bar	minor	
482	7-1	184.2	sand bar	minor	
483	7-1	184.4	erosion	band undercut	
484	7-1	184.5	sand bar	major	
485	7-1	184.7	sand bar	minor	
486	7-1	184.8	erosion	bank undercut	
487	7-1	185.2	erosion	bank undercut	
488	7-1	185.4	sand bar	minor	
489	7-1	185.7	erosion	bank undercut	
490	7-1	186.1	erosion	bank undercut	
491	7-1	186.3	erosion	bank undercut	
492	7-1	186.9	sand bar	minor	
493	7-1	187.2	erosion	bank undercut	
494	7-1	187.8	erosion	bank undercut	
495	7-1	188.5	sand bar	major	
496	7-1	189	erosion	bank undercut	
497	7-1	189.5	sand bar	major	
498	7-1	189.9	sand bar	major	
499	7-1	190.2	erosion	sand bar	
500	7-1	190.3	sand bar	minor	
501	7-1	190.8	sand bar	major	
502	7-1	190.9	erosion	bank undercut	
503	7-1	191.5	erosion	bank undercut	
504	7-1	191.7	sand bar	minor	
505	7-1	191.8	sand bar	minor	
506	7-1	192.1	sand bar	series of three	
507	7-1	192.2	sand bar	major; at mouth of stream	
508	7-1	192.5	erosion	bank undercut	
509	7-1	192.6	sand bar	major	
510	7-1	192.9	sand bar	major	
511	7-1	193.1	sand bar	major	
512	7-1	193.2	sand bar	minor	
513	7-1	194	sand bar	minor	
514	7-1	194.2	sand bar	major	
515	7-1	194.8	erosion	bank undercut	
516	7-1		sand bar	minor	
517	7-2	195.8	erosion	bank undercut	
518	7-2	195.9	sand bar	minor	
519	7-2	196.2	sand bar	minor	
520	7-2	196.4	sand bar	major	
521	7-2	196.5	erosion	bank undercut	

Table 1 (Continued)

Obstacle Number	Map Section (Pg.)	River Miles	Type of Obstruction	Description and Estimated Quantity	Notes
522	7-2	196.8	sand bar	major	
523	7-2	197	sand bar	major	
524	7-2	197.2	erosion	bank undercut	
525	7-2	197.5	sand bar	major	
526	7-2	197.6	sand bar	minor	
527	7-2	197.8	sand bar	major	
528	7-2	198.1	erosion	bank undercut	
529	7-2	198.5	sand bar	major	
530	7-2	198.7	erosion	bank undercut	
531	7-2	198.9	sand bar	minor	
532	7-2	199	sand bar	minor	
533	7-2	199.3	erosion	bank undercut	
534	7-2	199.8	sand bar	major	
535	7-2	200	erosion	exposed soil	
536	7-2	200.2	erosion	bank undercut	
537	7-2	201	erosion	bank undercut	
538	7-2	201.9	erosion	bank undercut	
539	7-2	202.6	erosion	bank undercut	
540	7-2	203	erosion	bank undercut	
541	7-2	203.3	sand bar	minor	
542	7-2	203.5	sand bar	major	
543	7-2	203.8	sand bar	major	
544	7-2	204.1	erosion	bank undercut	
545	7-2	204.2	erosion	bank undercut	
546	7-2	204.7	sand bar	minor	
547	7-2	204.8	sand bar	major	
548	7-2	204.9	sand bar	minor	
549	7-2	205	sand bar	major	
550	7-2	205.1	sand bar	minor	
551	7-2	205.2	erosion	exposed soil	
552	7-2	205.6	erosion	bank undercut	
553	7-2	206.1	erosion	bank undercut	
554	7-2	207.5	erosion	bank undercut	
555	7-2	207.8	sand bar	minor	
556	7-2	208.1	sand bars	major	series
557	7-2	208.5	sand bars	minor	series
558	7-2	208.6	erosion	bank undercut	
559	7-2	208.7	sand bar	minor	
560	7-2	208.8	erosion	exposed soil	
561	7-2	208.9	sand bar	minor	
562	7-2	209.4	sand bar	minor	
563	7-2	209.5	sand bar	minor	
564	7-2	209.6	erosion	exposed soil	
565	7-2	209.8	erosion	bank undercut	
566	7-2	210.1	sand bar	minor	

Table 1 (Continued)

Obstacle Number	Map Section (Pg.)	River Miles	Type of Obstruction	Description and Estimated Quantity	Notes
567	7-2	210.3	sand bar	minor	at mouth of stream
568	7-2	211	sand bar	major	by mouth of stream
569	7-2	211.3	erosion	bank undercut	

Table 2. Acreage of woodland per county.

County	Acreage
Yankton	1019
Hutchinson	692
Hansen	939
Davison	108
Sanborn	736

the Third Planning and Development District. The information will be utilized by them to obtain matching funds and grants to continue and expand existing programs to develop the lower James River basin. The information will also be used to emphasize the need for additional programs.

SUMMARY AND CONCLUSION

This project has shown that remotely sensed data can be a useful tool for river basin management.

For the most part, the data provided will be of assistance in evaluating many of the problems directly affecting the immediate river channel. Removal of the identified obstructions and prevention of future problems will greatly improve flow rate problems which is the long-term problem of the river.

Some of these problems were going to receive much more attention as a result of the proposed SCS Level B study of the lower James River watershed. Unfortunately, federal budget cutbacks have resulted in the postponement of the study indefinitely.

LITERATURE CITED

Schmucker, Paul, Nohr and Associates, 1974. Phase I - A project for Improvements Along the James River Within the Lower James Conservancy Sub-District. Schmucker, Paul, Nohr and Associates, Mitchell, South Dakota.

APPLICATION OF REMOTE SENSING IN THE NATIONAL MODEL IMPLEMENTATION PROGRAM, LAKE HERMAN WATERSHED

By

J. C. Eidenshink and F. A. Schmer

ABSTRACT

The Lake Herman watershed in southeastern South Dakota was selected as one of seven watersheds in the United States for involvement in the national pilot Model Implementation Program (MIP). Remote Sensing Institute is cooperating with numerous other states and local agencies to provide baseline and continuous resource information for watershed management. An information system including land cover, soil series, slope, drainage, and land treatment is being used to locate land in need of treatment, sites suitable for sediment control structures, estimate sediment delivery to the lake, and determine crop rotation practices.

APPLICATION OF REMOTE SENSING IN THE NATIONAL MODEL IMPLEMENTATION PROGRAM, LAKE HERMAN WATERSHED

By

Jeff Eidenshink and F. A. Schmer

INTRODUCTION

In 1978, the Lake Herman watershed near Madison, South Dakota was selected as one of seven water resource systems in the United States to participate in the national Model Implementation Program (MIP). MIP is a three year pilot cooperative program by the United States Department of Agriculture (USDA) and the United States Environmental Protection Agency (USEPA). The program is designed to test and evaluate various water quality improvement methods.

Several South Dakota groups are cooperating in the Lake Herman MIP program. They include: Lake Herman Development Association, First Planning and Development District, East Dakota Conservancy District, South Dakota Department of Natural Resource Development, South Dakota State University Extension Service, USDA Agricultural Stabilization and Conservation Service, USDA Soil Conservation Service (SCS), and the Remote Sensing Institue (RSI).

At the outset of the MIP, remote sensing techniques were employed as a means of monitoring land use and hydrologic changes throughout the watershed. In 1978 and 1979, NASA and SCS funded data collection and analysis and provided technical expertise for establishment of an inventory of the baseline condition of the watershed. SCS is the major user

of the data. Baseline landcover data for the 1978 and 1979 growing seasons and detailed soil survey data were coded into RSI's Area REsource Analysis System (AREAS), a computerized cellular information system (Wehde, 1979).

The data were analyzed to produce tabular and map information concerning location, quantity and severity of soil erosion (Myers et al. 1979). SCS requested maps and tabular data of many of the resource characteristics of the watershed. Two of the maps delineated land in need of treatment and areas suitable for sediment control structures.

Modeling of sediment delivery rates to Lake Herman was also undertaken in the second year of MIP. (Myers et al. 1980). Two basic approaches were investigated; one of which provided an estimate very similar to estimates obtained in other studies of Lake Herman.

The success of the first two years prompted SCS to increase their funding level of the project. SCS is funding nearly 90% of the third year activity. During the third year the modeling activities, the updating of the landcover and land treatment data, and other activities are continuing. This report is the culmination of a three-year involvement in the Lake Herman MIP.

PROCEDURES

Landcover

In July, 1980 low altitude 70 mm (1:61,000) color and color infrared aerial photography was collected for the Lake Herman watershed using the RSI aircraft. Ground truth data were obtained by recording the

landcover that occurred in each quadrant of road intersections within the watershed. Ground truth data for the watershed were collected at the time of the aerial data collection. The information was used to train interpreters and verify interpretation results.

The twelve basic landcover classes used in the previous years were interpreted on the 1980 imagery (Myers et al. 1980). The aerial photographs were enlarged to approximately 1:11,000 scale using an International Imaging System (I^2S) color additive viewer. The enlarged data were overlaid with a cellular grid on which each cell represented .25 hectares (.625 acres). Each cell was classified based on the category dominance within the cell.

Data Input

In the two previous years the landcover and the soils information were encoded into the computer manually in a slow and tedious method. The method ultimately presented many problems because of the numerous times the data were manually handled.

A new method of data input was developed and used to encode the 1980 landcover data into the computer. The new method was made possible through the upgrading of existing data processing equipment at RSI. Acquisition of a microprocessor with disk storage enabled the direct encoding of the land cover classification onto the magnetic disk. The data were encoded one square mile section at a time and each section was represented by a 32x32 grid matrix. Only boundaries or change points within the section were encoded.

An expanded matrix was displayed on a display monitor with each separate class within the section color coded (Figure 1). The operator then compared the section display with the gridded interpretation to verify that all boundaries and classes were correct. If any errors existed they were corrected through interactive re-entry of data points. Once corrected the section data were stored in disk memory in proper spatial relationship to other sections within the watershed. When all sections had been encoded the data for the entire watershed were reformatted to the AREAS format for mapping and analyses.

Land Treatment

Land treatment, specifically land treated with terraces, is a data component within the information system. As in the past, the data base was updated to include new treatment. The data were input utilizing the new entry system.

Sediment Delivery Modeling

A third modeling technique was investigated to determine if a better estimate of sediment delivery could be made. The third technique was a combination of the first two efforts (Myers, et al, 1980).

The third technique used was based on an assumption that both distance to the drainage point at which the sediment enters the drainage and the length of the drainage path to the lake should be weighted. The watershed was subdivided into 4 subwatersheds which corresponded to three tributaries entering the lake and the immediate lake shore (Figure 2).

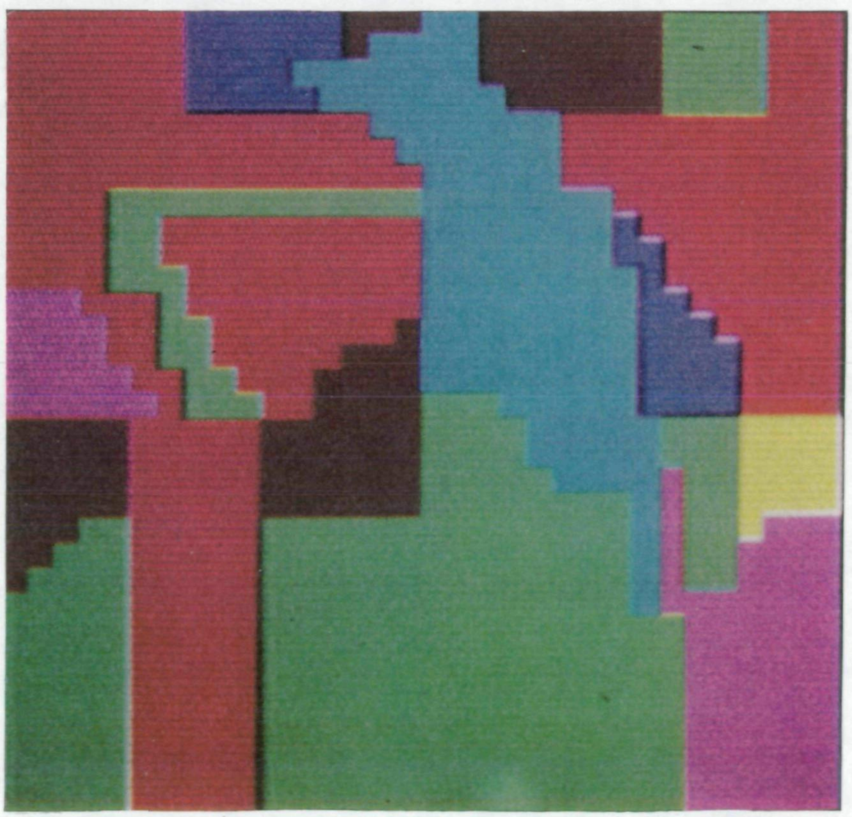

Figure 1. Color coded land use section (1 square mile) display.

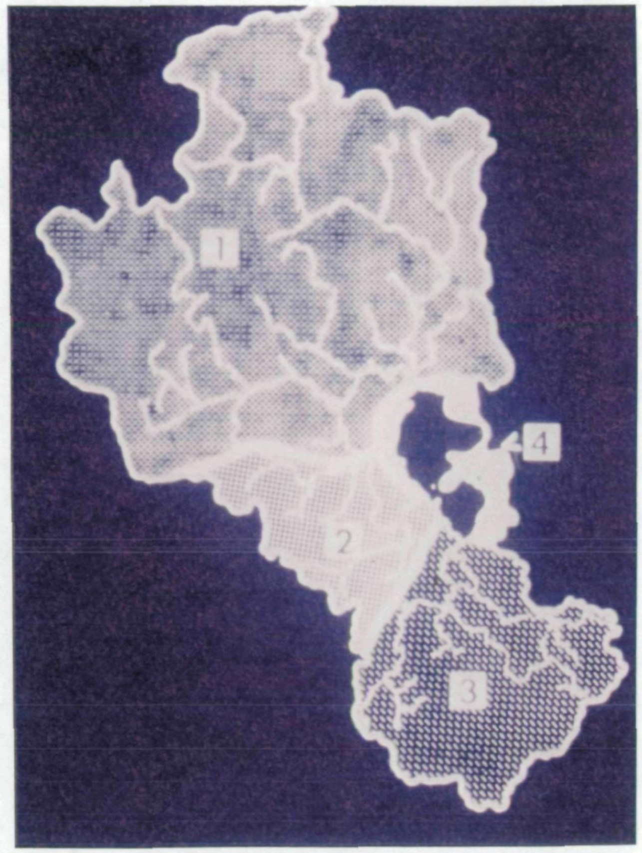

Figure 2. Subwatershed map.

The third model was run first assuming no existing land treatment and secondly with terraced land included. If capability class IVE land was terraced the calculation of sediment loss was based on the capability class IIIE values. Therefore, the assumption was that terracing improved the condition of the land by one capability class.

Crop Rotation

Landcover information had been derived for each of the three years of involvement in MIP. The landcover was analyzed to determine the crop rotation practices during that period. The information is very useful for evaluating soil loss because rotation is a major factor affecting soil loss over time.

The three landcover data bases were overlaid to determine the different rotation combinations. Some of the combination classes represented an insignificant percent of the total acreage within the watershed. The classes were the result of field border mis-alignment from year to year due to the cellularization process.

RESULTS AND DISCUSSION

New data input techniques were developed to encode the 1980 landcover and land treatment data bases. The technique was significantly faster and less expensive than the tedious techniques used previously.

The information system for the Lake Herman watershed now includes soils, slope drainage network, 3 consecutive years of landcover and of land treatment data bases.

The sediment modeling effort provided SCS with two results. First, the sediment delivery information for the proposed sediment control structures in the northern subwatershed was used to assist in evaluation of the effectiveness of each of the structures.

Model 1 was utilized to solve a major problem confronting the SCS. A major sediment control structure proposed by SCS for construction on the largest tributary area was estimated to cost $750,000. This cost greatly exceeded the available funding. Consequently, SCS was faced with locating another site for a sediment control structure. SCS requested that an abbreviated form of the sediment delivery model be used to assist in identifying the most effective site for a control structure from four alternate sites. The locations of the four alternate sites were plotted on a base map and the drainage area served by each site was also delineated on the map. The boundaries of the four areas were encoded into the computer.

The factors considered in the model were landcover, capability class IIE, IIIE and IVE and the SCS gross soil loss estimate for the capability classes based on the USLE. Tabulations of the total number of acres of each landcover type on each capability class were multiplied by the proper SCS gross soil loss estimate to derive a gross estimate of sediment delivery to each of the proposed control structures. SCS is using those data to determine the most cost effective control structure.

Secondly, the three weighted models provided comparative estimates of sediment delivery to the lake.

The basic parameters of the models were land cover type, capability class IIE, IIIE and IVE, SCS gross soil estimates based on the rainfall (R), erosion (K), slope and length (LS), vegetative cover (C), and management (P) factors of the universal soil loss equation (USLE) for each capability class and a weighting of those parameters based on the shortest distance to the lake or drainage entering the lake.

The first technique was based on the assumption that the further a parcel of land was from the lake the less sediment that parcel would deliver to the lake. So each parcel was weighted based on its distance to the lake. Figure 3 is a graphic representation of the weighting process for a portion of the watershed.

The second technique was based on the assumption that all sediment entering drainage would enter the lake. Each parcel of land was weighted based on its distance to drainage. Figure 4 is a graphic representation of the weighting process for a portion of the watershed.

The third technique used was based on an assumption that both distance to the drainage point at which the sediment enters the drainage and the distance of that point to the lake should be weighted. Figure 5 is a graphic representation of the third weighting process for a portion of the watershed. Each of the three models were run assuming no land treatment. However, the third model was also run with terraced land treatment included.

Comparison of the three models indicating that either model 1 or model 3 are the best estimators of sediment delivery according to the

Figure 3. Graphic representation of the weighting process for model 1.

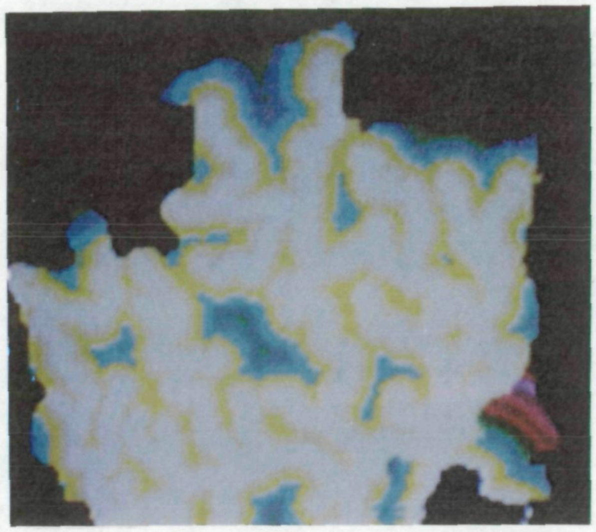

Figure 4. Graphic representation of the weighting process for model 2.

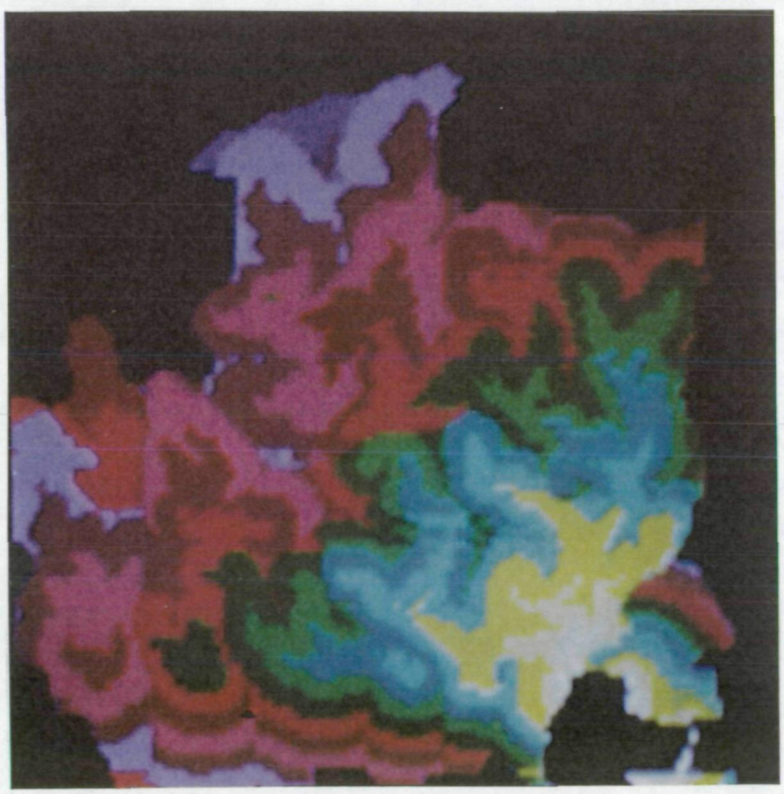

Figure 5. Graphic representation of the weighting process for model 3.

SCS. Table 1 shows the comparison of all three models and the model 3 run with land treatment considered.

Table 1. Comparison of three sediment delivery models.

Sub Watershed	Model 1	Model 2	Model 3 no treatment	Model 3 treatment
1	18.2	35.5	17.9	16.4
2	4.2	5.2	4.1	3.8
3	10.3	13.0	9.6	9.4
4	2.0	2.1	1.9	1.7
TOTAL	34.7	55.8	33.5	31.3

Discussion with SCS indicated that an estimate near 30 acre-feet annually was a realistic delivery rate. The estimate of Model 2 was considered extremely high.

The original intent was to use water quality sampling data to evaluate the accuracy of the models. Unfortunately, below normal snowfall and spring rain resulted in little or no runoff. The lack of runoff prevented any realistic evaluation of the model estimates.

The comparison between Model 3 treated and untreated indicates that the model does react to treatment changes. The inclusion of treatment reduced the sediment delivery by 2.2 acre feet or 6% for the entire watershed. In subwatershed, which is the largest, 12% of the land is treated. Model 3 with treatment included estimated an 8% reduction of sediment delivery.

The reaction to treatment indicates that Model 3 and perhaps Model 1 could be used to evaluate treatment efficiency. The evaluation should not be made without first calibrating and verifying the model estimates with ground data from water quality sampling.

Model 3 offers another (untested) potential advantage over Model 1. Model 3 uses drainage network data for calculation of path-to-lake. Sediment control structures which alter flow could be modeled in the drainage network data and benefit of the structure evaluated.

Table 2. Crop rotation sequences.

Rotation Sequence	%	Acres
Row crop - small grains - row crop	33.8	12487
Grass	23.8	8788
Small grains	23.0	1111
Row crop - row crop - small grains	12.2	4520
Other	10.8	3971
Row crop	10.5	3865
Row crop - small grains - small grains	5.9	2163
TOTAL	100.0	36905

Crop rotation sequences derived from three consecutive years of land cover data are presented in Table 2. These data indicate that the major sequence is a row crop-small grain rotation.

SUMMARY AND CONCLUSION

Over the past three years the information system has been developed, updated and used extensively for addressing several water quality problems. Early applications which included mapping and quantifying landcover, soils and terracing established the baseline condition of the watershed. Subsequent analysis identified land in need of treatment and potential sediment control structure sites.

The modeling techniques utilized input from the information system and the USLE to estimate sediment delivery to the lake as well as proposed sediment control structures. The modeling effort was not a complex procedure that involved extensive data collection. Instead the models utilize straightforward data base within the information system to provide believable, but not verified, estimates of sediment delivery.

If time had permitted, the data input to the models could have been refined further through the use of the information system. For instance, crop rotation patterns and specific erosion (K) factors for soils is already in the system. These two refinements could improve the reliability of the estimates.

The SCS and South Dakota Department of Water and Natural Resources (DWNR) realize the benefits of the procedures developed which utilize information system concepts. A joint proposal has been submitted by the SCS and DWNR for a similar water quality improvement effort in another South Dakota watershed. The proposal includes the development of an information system which will include the same data bases (soils, landcover, etc.) as the Lake Herman watershed information system. The new proposed project information system will include refined vegetative

cover and management practices data sets obtained from aerial photography. The additional data bases will be used to refine the modeling procedures already developed.

The results of the three-year MIP in the Lake Herman watershed have shown that remote sensing inputs to resource information systems are a valuable tool for management.

LITERATURE CITED

Wehde, Mike, B.K. Worcester, and K.J. Dalsted. 1979. Computerized resource management. Submitted to Journal of Soil and Water Conservation, Soil Conservation Society of America.

Myers, V. I., R.G. Best, K.J. Dalsted, M.E. DeVries, J.C. Eidenshink, J.L. Heilman, Ron Fowler, and F.A. Schmer. 1980. Remote sensing applications to resource problems in South Dakota. Annual Report to NASA, July 1, 1979-June 30, 1980. pp.103-115.